AIMS Mathematics, 10(11): 27581–27607.
DOI: 10.3934/math.20251213
Received: 25 August 2025
Revised: 08 November 2025
Accepted: 12 November 2025
Published: 26 November 2025

https://www.aimspress.com/journal/Math

Research article

Novel analytical approaches and stability examination for soliton solutions in a dispersive perturbed Gardner model

Wafaa B. Rabie[1], Hamdy M. Ahmed[2], A. M. Abd-Alla[3], Khadiga A. Ismail[4] and Ahmed Ramady[5,6,*]

[1] Department of Mathematics, Faculty of Science Luxor University, Taiba, Luxor, Egypt
[2] Department of Physics and Engineering Mathematics, Higher Institute of Engineering, El Shorouk Academy, Cairo, Egypt
[3] Department of Mathematics, Faculty of Science, University of Sohag, Sohag, Egypt
[4] Department of Clinical Laboratory Sciences, College of Applied Medical Sciences, Taif University, Taif 21944, Saudi Arabia
[5] GRC Department, The Applied College, King Abdulaziz University, Jeddah, 21589, Saudi Arabia
[6] Department of Mathematics and Computer Science, Faculty of Science, Beni-Suef University, Beni-Suef, Egypt

* **Correspondence:** Email: anasr@kau.edu.sa.

Abstract: This study presented a rigorous analytical investigation of the perturbed Gardner equation, a fundamental model describing nonlinear wave propagation in plasma physics, fluid dynamics, and nonlinear optics. Using an advanced analytical framework, we derived exact solutions capturing diverse wave behaviors: Localized bright solitons representing stable energy packets, dark solitons manifesting as intensity voids, singular solitons with distinctive phase profiles, and periodic waves governed by elliptic functions. Linear stability analysis revealed that solution robustness emerged from a delicate balance between nonlinear focusing and dispersive spreading, with precise parameter windows identified for maintaining structural integrity. A key finding identified the dispersion triplet—higher-order dispersion coefficients—as crucial for controlling wave amplitude, spectral broadening, and nonlinearity-dispersion balance. Numerical validation confirmed mathematical consistency and physical feasibility, with strong agreement between theory and simulations. This established a framework for understanding nonlinear wave phenomena in photonic and plasma applications.

Keywords: perturbed Gardner equation; soliton solutions; dispersion effects; stability analysis; nonlinear wave dynamics; analytical methods
Mathematics Subject Classification: 35G20, 35C07, 35C08, 35C09

1. Introduction

Nonlinear partial differential equations (NLPDEs) constitute a fundamental framework in mathematical modeling, enabling the characterization of complex dynamical behaviors that arise in physics, engineering, and numerous applied sciences [1–3]. Their remarkable capability to describe phenomena extending from quantum-scale interactions to large-scale astrophysical processes highlights their indispensable role in contemporary scientific inquiries [4–6]. In particular, NLPDEs that govern wave propagation, pattern formation, and fluid dynamics provide deep insights into the intrinsic nonlinear mechanisms shaping real-world systems [7–9]. Moreover, advanced models incorporating nonlinear interactions continue to enhance our understanding of diverse physical and engineering phenomena [10–12]. These developments collectively underscore the pivotal role of NLPDEs in advancing the theoretical and computational understanding of complex dynamical structures [13–15]. Recent studies, such as the work by Cao et al. [16] on Rossby waves in stratified fluids, demonstrate the continuing relevance of NLPDEs in understanding complex geophysical phenomena. Among these, evolution equations—particularly those describing wave dynamics—hold exceptional importance due to their widespread applications in theoretical and applied sciences [17–19]. A quintessential example is Gardner's equation [20], a hybrid of the Korteweg-de Vries (KdV) and modified KdV (mKdV) equations [21, 22]. This equation is pivotal in modeling stratified fluid waves, plasma physics, and nonlinear optical phenomena. When subjected to perturbations and higher-order dispersion effects—such as a dispersion triplet—it exhibits enriched dynamical behavior, though solving it analytically and assessing solution stability become formidable challenges [23, 24]. The pursuit of exact solutions for such equations is not merely a mathematical exercise but a gateway to unveiling underlying physical mechanisms [25, 26]. Closed-form solutions expose hidden symmetries and structures often obscured by numerical approximations. Equally vital is stability analysis, as only stable solutions correspond to observable, physically meaningful phenomena. Together, these facets define the forefront of nonlinear wave theory [27, 28]. Conventional methods like the inverse scattering transform are confined to integrable systems, while perturbation techniques hinge on small parameters that may not universally exist [29]. Such constraints have spurred the development of ansatz-based approaches, which accommodate broader classes of nonlinearities and dispersion terms [30]. Among these, the extended F-expansion method and its variants strike a balance between generality and tractability [31]. Yet, they falter for equations combining multiple nonlinearities and higher-order dispersion—precisely the case for the perturbed Gardner's equation with a dispersion triplet.

This study addresses a fundamental gap by pioneering an extended F-expansion method, specifically designed for complex nonlinear systems. For the first time, we apply this advanced technique to solve the perturbed Gardner's equation, expressed as [32]:

$$\mathfrak{Y}_t + \left(\rho_5\,\mathfrak{Y}^2 + \rho_1\,\mathfrak{Y}\right)\,\mathfrak{Y}_{\mathrm{x}} + \rho_4\,\mathfrak{Y}_{\mathrm{xtt}} + \rho_3\,\mathfrak{Y}_{\mathrm{xxt}} + \rho_2\,\mathfrak{Y}_{\mathrm{xxx}} - (\mathfrak{T}\,\mathfrak{Y}^m\mathfrak{Y}_{\mathrm{x}} + \mathcal{V}\,\mathfrak{Y}\mathfrak{Y}_{\mathrm{x}}\,\mathfrak{Y}_{\mathrm{xx}} + \mathfrak{S}\,\mathfrak{Y}_{\mathrm{x}}\mathfrak{Y}_{\mathrm{xx}} + \mathcal{J}\,\mathfrak{Y}_{\mathrm{x}}\,\mathfrak{Y}_{\mathrm{xxx}} + \mathcal{A}\,\mathfrak{Y}\,\mathfrak{Y}_{\mathrm{xxx}} + \mathcal{U}\,\mathfrak{Y}_{\mathrm{xxxxx}} + \mathcal{L}\,\mathfrak{Y}\,\mathfrak{Y}_{\mathrm{xxxxx}}) = 0. \tag{1.1}$$

Here, the wave amplitude is represented by $\mathfrak{Y}(\mathrm{x}, t)$, while ρ_1 denotes the linear advection coefficient, and ρ_5 governs quadratic nonlinearity. The terms $\rho_2 - \rho_4$ represent third-order dispersion effects (the dispersion triplet). The parameter $\mathfrak{T}$ controls the strength of the power-law perturbation, whereas $\mathcal{V}$ and $\mathfrak{S}$ describe cross-nonlinear interactions, and $\mathcal{J}$ and $\mathcal{A}$ model nonlinear dispersion coupling.

Finally, $\mathcal{U}$ and $\mathcal{L}$ account for fifth-order dispersion effects. In the investigated model, the dispersive perturbed Gardner equation, is of paramount importance in nonlinear science as it unifies the features of the KdV and modified KdV equations, thereby describing a broader spectrum of nonlinear wave phenomena. Its applications are vast and critical across various fields; in fluid dynamics, it models the propagation of internal waves in stratified oceans and shallow water surfaces, which is essential for understanding coastal erosion and tsunami dynamics. In plasma physics, it governs the behavior of ion-acoustic waves and non-Maxwellian plasmas. Furthermore, the model finds significant applications in nonlinear optics for describing pulse propagation in optical fibers, where dispersive and perturbation effects play a crucial role. Studying this model not only enhances our fundamental understanding of wave interactions and stability but also paves the way for practical advancements in wave energy harvesting, optical communication technologies, and atmospheric science. This comprehensive discussion of its importance and diverse applications underscores the novelty and relevance of our analytical and stability examination. This work is fundamentally motivated by the critical need to overcome the substantial limitations inherent in existing analytical approaches to the perturbed Gardner equation. While previous studies [28] successfully derived shock and solitary wave solutions using the G'/G-expansion method, this approach was inherently constrained by restrictive parameter requirements and could not adequately address higher-order dispersion effects or provide comprehensive stability analysis. These limitations have significantly hindered both theoretical progress and practical applications across fluid dynamics, plasma physics, and nonlinear optics. Our research directly addresses these challenges through the development of an innovative extended F-expansion framework that enables the systematic generation of unprecedented exact solution families encompassing localized waves, singular solitons, periodic structures, and exotic rational patterns; the complete incorporation of dispersion triplet effects and higher-order perturbations; and the establishment of a robust analytical-numerical validation protocol. This methodological advancement provides a unified platform for exploring nonlinearity-dispersion-perturbation interplay in Gardner-type systems, with demonstrated applications in plasma wave engineering and advanced optical communications, thereby bridging critical gaps between theoretical models and experimental realizations. In contrast, this research introduces a paradigm shift through the extended F-expansion method, which systematically generates an unprecedented range of exact solutions, including localized waves (e.g., bright/dark solitons), singular soliton solutions, periodic structures (such as elliptic functions, periodic waves, and singular periodic waves), and exotic wave patterns (including rational, hyperbolic, and exponential solutions). Moreover, this work fully incorporates the critical role of the dispersion triplet and establishes a robust analytical-numerical framework that simultaneously resolves three major challenges: precise treatment of perturbation terms and fifth-order dispersion effects, comprehensive stability analysis via phase-space diagnostics, and high-fidelity numerical verification of physical realizability. This advancement not only generalizes prior results as special cases but also provides a unified platform for exploring the interplay between nonlinearity, dispersion, and perturbation in Gardner-type systems, with demonstrated applications in plasma wave engineering and nonlinear optical communications.

This work is systematically organized to deliver a comprehensive understanding of the perturbed Gardner's equation and its solutions. In Section 2, we introduce the extended F-expansion method, detailing its mathematical framework and advantages over conventional techniques. Section 3 leverages advanced symbolic computation to derive new families of exact analytical solutions,

including solitons, periodic waves, and exotic wave patterns. The stability analysis in Section 4 rigorously quantifies critical stability thresholds and demonstrates how higher-order dispersion fundamentally modulates solution robustness, revealing previously unrecognized destabilization mechanisms. Section 5 brings these solutions to life through high-resolution 2D/3D visualizations, demonstrating their dynamic behavior under varying physical conditions. Finally, Section 6 synthesizes the key computational breakthroughs while outlining their implications for nonlinear wave theory and practical applications.

2. Advanced theoretical framework for the extended F-expansion method

This section establishes the rigorous mathematical foundations and systematic implementation protocol for the extended F-expansion method, a groundbreaking analytical technique for deriving exact solutions to NLPDEs. We demonstrate its universal applicability through the canonical NLPDE formulation [31]:

$$\mathcal{P}\left(\mathfrak{Y}, \mathfrak{Y}_{\mathrm{x}}, \mathfrak{Y}_{t}, \mathfrak{Y}_{\mathrm{xx}}, ...\right) = 0, \tag{2.1}$$

where $\mathcal{P}$ represents a polynomial functional of the physical field $\mathfrak{Y}(\mathrm{x}, t)$ and its partial derivatives. This formulation encapsulates the quintessential nonlinear dynamics governing wave phenomena across diverse physical systems.

The solution framework comprises several interconnected analytical procedures as follows:

Analytical procedure A. We establish the foundational analytical framework through the following wave solution ansatz:

$$\mathfrak{Y}(\mathrm{x}, t) = Z(\varepsilon), \quad \varepsilon = \mathrm{x} - \mathcal{G}t, \tag{2.2}$$

where $\mathcal{G}$ denotes the wave propagation velocity. This ansatz transforms the NPDE into an equivalent nonlinear ordinary differential equation (ODE) system through exact derivative conversion:

$$\mathcal{R}(Z, Z', Z'', Z''', \ldots) = 0. \tag{2.3}$$

Analytical procedure B. The solution architecture adopts a bidirectional series representation:

$$Z(\varepsilon) = \alpha_0 + \sum_{i=1}^{\mathbb{N}} \left[\alpha_i \mathcal{R}^i(\varepsilon) + \beta_i \mathcal{R}^{-i}(\varepsilon)\right], \tag{2.4}$$

where $\alpha_0, \alpha_i,$ and β_i are real coefficients constrained by the non-degeneracy condition $\alpha_N^2 + \beta_N^2 \neq 0$, ensuring solution nontrivially.

Analytical procedure C. The critical exponent $\mathbb{N}$ is determined through nonlinearity-derivative equilibrium analysis:

$$\mathcal{R}'(\varepsilon) = \epsilon \sqrt{\sum_{k=0}^{4} \varrho_k \mathcal{R}^k(\varepsilon)}, \tag{2.5}$$

where ϱ_k are real coefficients and $\epsilon = \pm 1$ governs that the balancing constant $\mathbb{N}$ is systematically determined through rigorous application of the homogeneous balance principle (BP). This fundamental procedure involves careful scaling analysis of the governing equation (Eq (2.4)), where we establish exact equivalence between the dominant nonlinear term (e.g., $\mathcal{R}^p$) and the highest-order

derivative (e.g., $\mathcal{R}^{(m)}$). The resulting balance equation $N + m = p\,N$ provides an exact algebraic relation that uniquely specifies the value of N.

Analytical procedure D. Substitution yields the characteristic polynomial system:

$$\sum_{j=0}^{15} \gamma_j \mathcal{R}^j(\varepsilon) = 0, \text{ and } \sum_{i=1}^{19} \frac{s_i\,\mathcal{R}^i(\varepsilon)}{\mathcal{R}'(\varepsilon)} = 0.$$

Enforcing the annihilation conditions $\gamma_j \equiv 0$ and $s_i \equiv 0$ generates a nonlinear algebraic system, and symbolic computation of this system produces exact parameter constraints, novel soliton solution families, and complete classification of wave behaviors. This four-pillar architecture establishes a comprehensive analytical engine for nonlinear wave theory, combining mathematical rigor with computational tractability to unlock previously inaccessible solution classes. While the extended F-expansion method provides a powerful analytical framework for solving NPDEs, several inherent limitations define its operational boundaries and scope of applicability. The bidirectional series representation in Eq (2.4) inherently constrains the solution space to functional forms expressible through the auxiliary function $\mathcal{R}(\varepsilon)$. The diversity of obtainable solutions is intrinsically governed by the chosen auxiliary ODE (Eq (2.5)). While we selected the most general form compatible with our model, this dependency fundamentally limits the solution spectrum to patterns derivable from the auxiliary equation's solution family. The homogeneous balance principle used to determine $\mathbb{N}$ relies on dominant term analysis, which may become ambiguous for equations with multiple competing nonlinearities or when the highest-order derivative coefficient contains the dependent variable. The finite series truncation at order $\mathbb{N}$, while computationally necessary, imposes an upper bound on solution complexity. Higher-order nonlinear phenomena or intricate wave interactions requiring infinite series representations may not be fully captured within this truncated framework. Unlike systematic approaches like the inverse scattering transform applicable to completely integrable systems, this method operates within a predetermined solution space, making it less suitable for strongly non-integrable systems or those requiring complete integrability analysis. Despite these methodological constraints, the extended F-expansion method remains exceptionally valuable for its systematic generation of broad solution families in non-integrable systems where more rigorous approaches are inapplicable. The framework's strength lies in its ability to provide exact analytical solutions with clear physical interpretations, bridging the gap between abstract mathematical models and observable wave phenomena. These limitations also suggest productive directions for future methodological enhancements, including hybrid analytical-numerical approaches and adaptive ansatz formulations.

3. Exact analytical solutions for the generalized Gardner's equation

Through systematic application of the traveling wave transformation Eq (2.2) with the critical parameter specification $m = 1$, we rigorously reduce the perturbed Gardner's equation (Eq 1.1) to its canonical nonlinear ODE representation. The detailed derivation proceeds as follows: First, we substitute the traveling wave ansatz $\mathfrak{Y}(\mathrm{x}, t) = Z(\varepsilon)$ with $\varepsilon = \mathrm{x} - \mathcal{G}\,t$ into Eq (1.1). This transformation converts all partial derivatives into ordinary derivatives with respect to ε, where $\mathfrak{Y}_t = -\mathcal{G}\,Z'$, $\mathfrak{Y}_{\mathrm{x}} = Z'$, $\mathfrak{Y}_{\mathrm{xxx}} = Z^{(3)}$, and $\mathfrak{Y}_{\mathrm{xxxxx}} = Z^{(5)}$. The parameter $m = 1$ in the original model represents a specific nonlinearity exponent that significantly simplifies the equation structure. Next, we apply the boundary

condition that $Z^{(n)} \to 0$ as $|\varepsilon| \to \infty$ for all $n \geq 1$. This process, combined with the specific value $m = 1$, allows us to obtain the simplified NLODE form representation:

$$-(\mathcal{L}\, Z + \mathcal{U})\, Z^{(5)} + \left[-\mathcal{A}\, Z + \left(\mathcal{G}^2\, \rho_4 - \mathcal{G}\, \rho_3 + \rho_2\right) - \mathcal{J}\, Z'\right] Z^{(3)} - \mathcal{V} Z Z' Z'' + (\rho_1 - \mathfrak{T})\; Z\, Z' +$$

$$\rho_5 Z^2 Z' - \mathfrak{S} Z' Z'' - \mathcal{G} Z' = 0. \tag{3.1}$$

To solve Eq (3.1), we employ the solution architecture defined in Eq (2.4) with $\mathbb{N} = 2$, which represents a bidirectional series expansion. The specific form of our solution is obtained by:

$$Z = \alpha_0 + \alpha_1\, \mathcal{R}(\varepsilon) + \alpha_2\, \mathcal{R}^2(\varepsilon) + \frac{\beta_1}{\mathcal{R}(\varepsilon)} + \frac{\beta_2}{\mathcal{R}^2(\varepsilon)}. \tag{3.2}$$

The real-valued coefficients α_i $(i = 0, 1, 2)$ and β_j $(j = 1, 2)$ are rigorously determined through the non-degeneracy constraint $\alpha_2^2 + \beta_2^2 \neq 0$, ensuring nontrivial solutions. Through systematic substitution of the ansatz Eq (3.2) with the auxiliary condition Eq (2.5) into the governing equation (Eq (3.1)), we obtain a characteristic polynomial in $\mathcal{R}(\varepsilon)$ under the parameter constraints $\beta_1 = \alpha_0 = \alpha_1 = 0$. By enforcing exact coefficient cancellation for each power of $\mathcal{R}(\varepsilon)$, we derive a coupled nonlinear algebraic system. Through advanced symbolic computation in Wolfram Mathematica, we rigorously derive the following fundamental solution classes that satisfy the system exactly:

First case. Under the constraints $\varrho_1 = \varrho_3 = 0$, the algebraic system undergoes a fundamental transformation, resulting in a solution space defined by:

(1.1) $\beta_2 = 0,\ \ \alpha_2 = \frac{3\, \varrho_4\, [(2\, \mathcal{A}+\mathfrak{S}) \pm \sqrt{(2\, \mathcal{A}+\mathfrak{S})^2 + 40\, \rho_5\, \mathcal{U}}]}{\rho_5},\ \ \mathcal{V} = \frac{\mathcal{L}\left(\varrho_0 (2\mathcal{A}+\mathfrak{S}) \pm \sqrt{\varrho_0^2 \left((2\mathcal{A}+\mathfrak{S})^2 + 40\rho_5 \mathcal{U}\right)}\right)}{2\mathcal{U}\varrho_0},$

$$\mathcal{J} = 0,\ \ \rho_4 = \frac{\left(6\varrho_0\, \varrho_4 (\mathfrak{S}(2\, \mathcal{A}+\mathfrak{S}) + 12\rho_5\, \mathcal{U}) \mp 6\, \mathfrak{S}\, \varrho_4 \sqrt{\varrho_0^2 \left((2\, \mathcal{A}+\mathfrak{S})^2 + 40\, \rho_5\, \mathcal{U}\right)}\right) + \rho_5 (4\, \varrho_2\, (\mathcal{G}\, \rho_3 - \rho_2 + 4\mathcal{U}\, \varrho_2) + \mathcal{G})}{4\mathcal{G}^2\, \rho_5 \varrho_2},$$

$$\rho_1 = \tfrac{1}{40\mathcal{U}\, \varrho_0\, \varrho_2}\, (\varrho_0 [\mathcal{G}(2\mathcal{A} + \mathfrak{S}) + 8\mathcal{U}(-9\varrho_4 \sqrt{\varrho_0^2\, ((2\mathcal{A} + \mathfrak{S})^2 + 40\rho_5 \mathcal{U})} + 4\varrho_2^2\, (\mathcal{A} + 20\mathcal{L}\varrho_2 + 3\, \mathfrak{S}) +$$
$$5\, \mathfrak{T}\, \varrho_2)] + [24\, \mathcal{U}\, \varrho_0^2\, \varrho_4\, (6\mathcal{A} - 80\, \mathcal{L}\, \varrho_2 - 7\mathfrak{S}) \mp \left(\mathcal{G} - 64\, \mathcal{U}\, \varrho_2^2\right) \sqrt{\varrho_0^2\, ((2\, \mathcal{A} + \mathfrak{S})^2 + 40\, \rho_5\, \mathcal{U})}]).$$

(1.2) $\beta_2 = \frac{3\left(\varrho_0 (2\mathcal{A}+\mathfrak{S}) \pm \sqrt{\varrho_0^2 \left((2\mathcal{A}+\mathfrak{S})^2 + 40\rho_5 \mathcal{U}\right)}\right)}{\rho_5},\ \ \alpha_2 = 0,\ \ \mathcal{V} = \frac{\mathcal{L}\left(\varrho_0 (2\mathcal{A}+\mathfrak{S}) \pm \sqrt{\varrho_0^2 \left((2\mathcal{A}+\mathfrak{S})^2 + 40\rho_5 \mathcal{U}\right)}\right)}{2\mathcal{U}\varrho_0},$

$$\mathcal{J} = 0,\ \ \rho_4 = \frac{\left(6\varrho_0\, \varrho_4\, (\mathfrak{S}(2\, \mathcal{A}+\mathfrak{S}) + 12\, \rho_5\, \mathcal{U}) \mp 6\, \mathfrak{S} \varrho_4 \sqrt{\varrho_0^2\, \left((2\mathcal{A}+\mathfrak{S})^2 + 40\, \rho_5\, \mathcal{U}\right)}\right) + \rho_5 (4\, \varrho_2 (\mathcal{G}\, \rho_3 - \rho_2 + 4\mathcal{U}\, \varrho_2) + \mathcal{G})}{4\mathcal{G}^2\, \rho_5 \varrho_2},$$

$$\rho_1 = \tfrac{1}{40\, \mathcal{U}\, \varrho_0\, \varrho_2} [\varrho_0 (\mathcal{G}(2\mathcal{A} + \mathfrak{S}) + 8\mathcal{U} \left(-9\varrho_4 \sqrt{\varrho_0^2\, ((2\mathcal{A} + \mathfrak{S})^2 + 40\rho_5 \mathcal{U})} + 4\varrho_2^2 (\mathcal{A} + 20\, \mathcal{L}\, \varrho_2 + 3\, \mathfrak{S}\right) +$$
$$5\, \mathfrak{T}\, \varrho_2)) + (24\, \mathcal{U}\, \varrho_0^2\, \varrho_4\, (6\, \mathcal{A} - 80\, \mathcal{L}\, \varrho_2 - 7\, \mathfrak{S}) \mp (\mathcal{G} - 64\, \mathcal{U}\, \varrho_2^2) \sqrt{\varrho_0^2 [(2\, \mathcal{A} + \mathfrak{S})^2 + 40\, \rho_5\, \mathcal{U}]})].$$

From the previously derived solution set (1.1), we derive exact solutions to Eq (1.1) having the following general form:

(1.1.1) Considering the free parameters and their restrictions: The model structure parameters are fixed as $\varrho_0 = 1,\ \varrho_2 = -m^2 - 1,\ \varrho_4 = m^2$; the elliptic modulus parameter must satisfy $0 < m \leq 1$ to ensure well-defined periodic solutions; the nonlinear coefficient requires $\rho_5 \neq 0$ to avoid solution

singularity; the amplitude parameters $\mathcal{A}$, $\mathfrak{S}$, and $\mathcal{U}$ must satisfy $(2\mathcal{A}+\mathfrak{S})^2+40\,\rho_5\,\mathcal{U}>0$ to guarantee real-valued solutions, while the wave velocity $\mathcal{G}$ is a free real parameter ($\mathcal{G}\in\mathbb{R}$), and the sign choice ± generates two distinct solution branches. Under these conditions, the JEF solutions take the following form:

$$\mathfrak{Y}_{1.1.1}=-\frac{3\,m^2}{\rho_5}\left[\left(\mathfrak{S}\pm\sqrt{(2\,\mathcal{A}+\mathfrak{S})^2+40\,\rho_5\,\mathcal{U}}\right)+2\,\mathcal{A}\right]\,\mathrm{sn}^2\left[\mathrm{x}-\mathcal{G}\,t\right], \tag{3.3}$$

or

$$\mathfrak{Y}_{1.1.2}=-\frac{3\,m^2}{\rho_5}\left[\left(\mathfrak{S}\pm\sqrt{(2\,\mathcal{A}+\mathfrak{S})^2+40\,\rho_5\,\mathcal{U}}\right)+2\,\mathcal{A}\right]\,\mathrm{cd}^2\left[\mathrm{x}-\mathcal{G}\,t\right]. \tag{3.4}$$

Setting $m=1$ in Eq (3.3) yields the dark soliton solution:

$$\mathfrak{Y}_{1.1.1,1}=-\frac{3}{\rho_5}\left[\left(\mathfrak{S}\pm\sqrt{(2\,\mathcal{A}+\mathfrak{S})^2+40\,\rho_5\,\mathcal{U}}\right)+2\,\mathcal{A}\right]\,\tanh^2\left[\mathrm{x}-\mathcal{G}\,t\right]. \tag{3.5}$$

(1.1.2) Considering the free parameters and their restrictions: The model structure parameters are fixed as $\varrho_0=1-m^2$, $\varrho_2=m^2-1$, $\varrho_4=-m^2$; the elliptic modulus parameter must satisfy $0<m\leq 1$ to ensure well-defined periodic solutions; the nonlinear coefficient requires $\rho_5\neq 0$ to avoid solution singularity; the amplitude parameters $\mathcal{A}$, $\mathfrak{S}$, and $\mathcal{U}$ must satisfy $(2\,\mathcal{A}+\mathfrak{S})^2+40\,\rho_5\,\mathcal{U}>0$ to guarantee real-valued solutions, while the wave velocity $\mathcal{G}$ is a free real parameter ($\mathcal{G}\in\mathbb{R}$), and the sign choice ± generates two distinct solution branches. Under these conditions, the JEF solutions take the following form:

$$\mathfrak{Y}_{1.1.3}=-\frac{-3\,m^2}{\rho_5}\left[\mathfrak{S}+2\,\mathcal{A}\pm\sqrt{(2\,\mathcal{A}+\mathfrak{S})^2+40\,\rho_5\,\mathcal{U}}\right]\,\mathrm{cn}^2\left[\mathrm{x}-\mathcal{G}\,t\right]. \tag{3.6}$$

Setting $m=1$ in Eq (3.6) yields the bright soliton solution:

$$\mathfrak{Y}_{1.1.3,1}=-\frac{3}{\rho_5}\left[\left(\mathfrak{S}\pm\sqrt{(2\,\mathcal{A}+\mathfrak{S})^2+40\,\rho_5\,\mathcal{U}}\right)+2\,\mathcal{A}\right]\,\mathrm{sech}^2\left[\mathrm{x}-\mathcal{G}\,t\right]. \tag{3.7}$$

(1.1.3) Considering the free parameters and their restrictions: The model structure parameters are fixed as $\varrho_0=m^2-1$, $\varrho_2=2-m^2$, $\varrho_4=-1$; the elliptic modulus parameter must satisfy $0\leq m\leq 1$ to ensure well-defined periodic solutions; the nonlinear coefficient requires $\rho_5\neq 0$ to avoid solution singularity; the amplitude parameters $\mathcal{A}$, $\mathfrak{S}$, and $\mathcal{U}$ must satisfy $(2\,\mathcal{A}+\mathfrak{S})^2+40\,\rho_5\,\mathcal{U}>0$ to guarantee real-valued solutions, while the wave velocity $\mathcal{G}$ is a free real parameter ($\mathcal{G}\in\mathbb{R}$), and the sign choice ± generates two distinct solution branches. Under these conditions, the JEF solutions take the following form:

$$\mathfrak{Y}_{1.1.4}=-\frac{3}{\rho_5}\left[\left(\mathfrak{S}\pm\sqrt{(2\,\mathcal{A}+\mathfrak{S})^2+40\,\rho_5\,\mathcal{U}}\right)+2\,\mathcal{A}\right]\,\mathrm{dn}^2\left[\mathrm{x}-\mathcal{G}\,t\right]. \tag{3.8}$$

Setting $m=1$ in Eq (3.8) yields the bright soliton solution:

$$\mathfrak{Y}_{1.1.4,1}=-\frac{3}{\rho_5}\left[\left(\mathfrak{S}\pm\sqrt{(2\,\mathcal{A}+\mathfrak{S})^2+40\,\rho_5\,\mathcal{U}}\right)+2\,\mathcal{A}\right]\,\mathrm{sech}^2\left[\mathrm{x}-\mathcal{G}\,t\right]. \tag{3.9}$$

(1.1.4) Considering the free parameters and their restrictions: The model structure parameters are fixed as $\varrho_0 = m^2$, $\varrho_2 = -(m^2+1)$, $\varrho_4 = 1$; the elliptic modulus parameter must satisfy $0 \leq m \leq 1$ to ensure well-defined periodic solutions; the nonlinear coefficient requires $\rho_5 \neq 0$ to avoid solution singularity; the amplitude parameters $\mathcal{A}$, $\mathfrak{S}$, and $\mathcal{U}$ must satisfy $(2\mathcal{A}+\mathfrak{S})^2 + 40\,\rho_5\,\mathcal{U} > 0$ to guarantee real-valued solutions, while the wave velocity $\mathcal{G}$ is a free real parameter ($\mathcal{G} \in \mathbb{R}$), and the sign choice ± generates two distinct solution branches. Under these conditions, the JEF solutions take the following form:

$$\mathfrak{Y}_{1.1.5} = -\frac{3}{\rho_5}\left[\left(\mathfrak{S} \pm \sqrt{(2\,\mathcal{A}+\mathfrak{S})^2 + 40\,\rho_5\,\mathcal{U}}\right) + 2\,\mathcal{A}\right]\,\mathrm{ns}^2\left[\mathrm{x} - \mathcal{G}\,t\right], \tag{3.10}$$

or

$$\mathfrak{Y}_{1.1.6} = -\frac{3}{\rho_5}\left[\left(\mathfrak{S} \pm \sqrt{(2\,\mathcal{A}+\mathfrak{S})^2 + 40\,\rho_5\,\mathcal{U}}\right) + 2\,\mathcal{A}\right]\,\mathrm{ns}^2\left[\mathrm{x} - \mathcal{G}\,t\right]. \tag{3.11}$$

Setting $m = 1$ in Eq (3.10) yields the bright soliton solution:

$$\mathfrak{Y}_{1.1.5,1} = \frac{3}{\rho_5}\left[\left(\mathfrak{S} \pm \sqrt{(2\,\mathcal{A}+\mathfrak{S})^2 + 40\,\rho_5\,\mathcal{U}}\right) + 2\,\mathcal{A}\right]\,\coth^2\left[\mathrm{x} - \mathcal{G}\,t\right]. \tag{3.12}$$

Setting $m = 0$ in Eqs (3.10) and (3.11) yields the singular periodic solutions:

$$\mathfrak{Y}_{1.1.5,2} = \frac{3}{\rho_5}\left[\left(\mathfrak{S} \pm \sqrt{(2\,\mathcal{A}+\mathfrak{S})^2 + 40\,\rho_5\,\mathcal{U}}\right) + 2\,\mathcal{A}\right]\,\csc^2\left[\mathrm{x} - \mathcal{G}\,t\right], \tag{3.13}$$

or

$$\mathfrak{Y}_{1.1.6,1} = \frac{3}{\rho_5}\left[\left(\mathfrak{S} \pm \sqrt{(2\,\mathcal{A}+\mathfrak{S})^2 + 40\,\rho_5\,\mathcal{U}}\right) + 2\,\mathcal{A}\right]\,\sec^2\left[\mathrm{x} - \mathcal{G}\,t\right]. \tag{3.14}$$

(1.1.5) Considering the free parameters and their restrictions: The model structure parameters are fixed as $\varrho_0 = -m^2$, $\varrho_2 = 2\,m^2 - 1$, $\varrho_4 = 1 - m^2$; the elliptic modulus parameter must satisfy $0 \leq m < 1$ to ensure well-defined periodic solutions; the nonlinear coefficient requires $\rho_5 \neq 0$ to avoid solution singularity; the amplitude parameters $\mathcal{A}$, $\mathfrak{S}$, and $\mathcal{U}$ must satisfy $(2\,\mathcal{A}+\mathfrak{S})^2 + 40\,\rho_5\,\mathcal{U} > 0$ to guarantee real-valued solutions, while the wave velocity $\mathcal{G}$ is a free real parameter ($\mathcal{G} \in \mathbb{R}$), and the sign choice ± generates two distinct solution branches. Under these conditions, the JEF solutions take the following form:

$$\mathfrak{Y}_{1.1.7} = -\frac{3\,(1-m^2)}{\rho_5}\left[\left(\mathfrak{S} \pm \sqrt{(2\,\mathcal{A}+\mathfrak{S})^2 + 40\,\rho_5\,\mathcal{U}}\right) + 2\,\mathcal{A}\right]\,\mathrm{nc}^2\left[\mathrm{x} - \mathcal{G}\,t\right]. \tag{3.15}$$

Setting $m = 0$ in Eq (3.15) yields the singular periodic solution:

$$\mathfrak{Y}_{1.1.7,1} = \frac{3}{\rho_5}\left[\left(\mathfrak{S} \pm \sqrt{(2\,\mathcal{A}+\mathfrak{S})^2 + 40\,\rho_5\,\mathcal{U}}\right) + 2\,\mathcal{A}\right]\,\csc^2\left[\mathrm{x} - \mathcal{G}\,t\right]. \tag{3.16}$$

(1.1.6) Considering the free parameters and their restrictions: The model structure parameters are fixed as $\varrho_0 = 1$, $\varrho_2 = 2 - m^2$, $\varrho_4 = 1 - m^2$; the elliptic modulus parameter must satisfy $0 \leq m < 1$ to ensure well-defined periodic solutions; the nonlinear coefficient requires $\rho_5 \neq 0$ to avoid solution singularity; the amplitude parameters $\mathcal{A}$, $\mathfrak{S}$, and $\mathcal{U}$ must satisfy $(2\mathcal{A}+\mathfrak{S})^2 + 40\rho_5\mathcal{U} > 0$ to guarantee real-valued solutions, while the wave velocity $\mathcal{G}$ is a free real parameter ($\mathcal{G} \in \mathbb{R}$),

and the sign choice ± generates two distinct solution branches. Under these conditions, the JEF solutions take the following form:

$$\mathfrak{Y}_{1.1.8} = -\frac{3\,(1-m^2)}{\rho_5}\left[\left(\mathfrak{S} \pm \sqrt{(2\,\mathcal{A}+\mathfrak{S})^2+40\,\rho_5\,\mathcal{U}}\right)+2\,\mathcal{A}\right]\,\mathrm{sc}^2\left[\mathrm{x}-\mathcal{G}\,t\right]. \tag{3.17}$$

Setting $m = 0$ in Eq (3.17) yields the singular periodic solution:

$$\mathfrak{Y}_{1.1.8,1} = \frac{3}{\rho_5}\left[\left(\mathfrak{S} \pm \sqrt{(2\,\mathcal{A}+\mathfrak{S})^2+40\,\rho_5\,\mathcal{U}}\right)+2\,\mathcal{A}\right]\,\tan^2\left[\mathrm{x}-\mathcal{G}\,t\right]. \tag{3.18}$$

(1.1.7) Considering the free parameters and their restrictions: the model structure parameters are fixed as $\varrho_0 = 1-m^2$, $\varrho_2 = 2-m^2$, $\varrho_4 = 1$; the elliptic modulus parameter must satisfy $0 \le m \le 1$ to ensure well-defined periodic solutions; the nonlinear coefficient requires $\rho_5 \neq 0$ to avoid solution singularity the amplitude parameters $\mathcal{A}$, $\mathfrak{S}$, and $\mathcal{U}$ must satisfy $(2\,\mathcal{A}+\mathfrak{S})^2+40\,\rho_5\,\mathcal{U} > 0$ to guarantee real-valued solutions, while the wave velocity $\mathcal{G}$ is a free real parameter ($\mathcal{G} \in \mathbb{R}$), and the sign choice ± generates two distinct solution branches. Under these conditions, the JEF solutions take the following form:

$$\mathfrak{Y}_{1.1.9} = -\frac{3}{\rho_5}\left[\left(\mathfrak{S} \pm \sqrt{(2\,\mathcal{A}+\mathfrak{S})^2+40\,\rho_5\,\mathcal{U}}\right)+2\,\mathcal{A}\right]\,\mathrm{cs}^2\left[\mathrm{x}-\mathcal{G}\,t\right]. \tag{3.19}$$

Setting $m = 1$ or $m = 0$ in Eq (3.19) yields the singular soliton solution, or periodic solution:

$$\mathfrak{Y}_{1.1.9,1} = \frac{3}{\rho_5}\left[\left(\mathfrak{S} \pm \sqrt{(2\,\mathcal{A}+\mathfrak{S})^2+40\,\rho_5\,\mathcal{U}}\right)+2\,\mathcal{A}\right]\,\mathrm{csch}^2\left[\mathrm{x}-\mathcal{G}\,t\right], \tag{3.20}$$

or

$$\mathfrak{Y}_{1.1.9,2} = \frac{3}{\rho_5}\left[\left(\mathfrak{S} \pm \sqrt{(2\,\mathcal{A}+\mathfrak{S})^2+40\,\rho_5\,\mathcal{U}}\right)+2\,\mathcal{A}\right]\,\cot^2\left[\mathrm{x}-\mathcal{G}\,t\right]. \tag{3.21}$$

(1.1.8) Considering the free parameters and their restrictions: The model structure parameters are fixed as $\varrho_0 = 1-m^2(1-m^2)$, $\varrho_2 = 2m^2-1$, $\varrho_4 = 1$; the elliptic modulus parameter must satisfy $0 \le m \le 1$ to ensure well-defined periodic solutions; the nonlinear coefficient requires $\rho_5 \neq 0$ to avoid solution singularity; the amplitude parameters $\mathcal{A}$, $\mathfrak{S}$, and $\mathcal{U}$ must satisfy $(2\mathcal{A}+\mathfrak{S})^2+40\rho_5\mathcal{U} > 0$ to guarantee real-valued solutions, while the wave velocity $\mathcal{G}$ is a free real parameter ($\mathcal{G} \in \mathbb{R}$), and the sign choice ± generates two distinct solution branches. Under these conditions, the JEF solutions take the following form:

$$\mathfrak{Y}_{1.1.10} = -\frac{3}{\rho_5}\left[\left(\mathfrak{S} \pm \sqrt{(2\,\mathcal{A}+\mathfrak{S})^2+40\,\rho_5\,\mathcal{U}}\right)+2\,\mathcal{A}\right]\,\mathrm{sd}^2\left[\mathrm{x}-\mathcal{G}\,t\right]. \tag{3.22}$$

Setting $m = 1$ or $m = 0$ in Eq (3.22) yields the hyperbolic solution, or periodic solution:

$$\mathfrak{Y}_{1.1.10,1} = \frac{3}{\rho_5}\left[\left(\mathfrak{S} \pm \sqrt{(2\,\mathcal{A}+\mathfrak{S})^2+40\,\rho_5\,\mathcal{U}}\right)+2\,\mathcal{A}\right]\,\sinh^2\left[\mathrm{x}-\mathcal{G}\,t\right], \tag{3.23}$$

or

$$\mathfrak{Y}_{1.1.10,2} = \frac{3}{\rho_5}\left[\left(\mathfrak{S} \pm \sqrt{(2\,\mathcal{A}+\mathfrak{S})^2+40\,\rho_5\,\mathcal{U}}\right)+2\,\mathcal{A}\right]\,\sin^2\left[\mathrm{x}-\mathcal{G}\,t\right]. \tag{3.24}$$

(1.1.9) Considering the free parameters and their restrictions: The model structure parameters are fixed as $\varrho_0 = \frac{1}{4}$, $\varrho_2 = \frac{1-2m^2}{2}$, $\varrho_4 = \frac{1}{4}$; the elliptic modulus parameter must satisfy $0 \leq m \leq 1$ to ensure well-defined periodic solutions; the nonlinear coefficient requires $\rho_5 \neq 0$ to avoid solution singularity; the amplitude parameters $\mathcal{A}$, $\mathfrak{S}$, and $\mathcal{U}$ must satisfy $(2\mathcal{A} + \mathfrak{S})^2 + 40\rho_5\mathcal{U} > 0$ to guarantee real-valued solutions, while the wave velocity $\mathcal{G}$ is a free real parameter ($\mathcal{G} \in \mathbb{R}$), and the sign choice ± generates two distinct solution branches. Under these conditions, the JEF solutions take the following form:

$$\mathfrak{Y}_{1.1.11} = -\frac{3}{\rho_5}\left[\left(\mathfrak{S} \pm \sqrt{(2\,\mathcal{A} + \mathfrak{S})^2 + 40\,\rho_5\,\mathcal{U}}\right) + 2\,\mathcal{A}\right]\,(\mathrm{cs}\,[\mathrm{x} - \mathcal{G}\,t] \pm \mathrm{nd}\,[\mathrm{x} - \mathcal{G}\,t])^2. \quad (3.25)$$

Setting $m = 1$ or $m = 0$ in Eq (3.25) yields the hyperbolic solution, or singular periodic solution:

$$\mathfrak{Y}_{1.1.11,1} = \frac{3}{\rho_5}\left[\left(\mathfrak{S} \pm \sqrt{(2\,\mathcal{A} + \mathfrak{S})^2 + 40\,\rho_5\,\mathcal{U}}\right) + 2\,\mathcal{A}\right]\,(\cosh\,[\mathrm{x} - \mathcal{G}\,t] \pm \mathrm{csch}\,[\mathrm{x} - \mathcal{G}\,t])^2, \quad (3.26)$$

or

$$\mathfrak{Y}_{1.1.11,2} = \frac{3}{\rho_5}\left[\left(\mathfrak{S} \pm \sqrt{(2\,\mathcal{A} + \mathfrak{S})^2 + 40\,\rho_5\,\mathcal{U}}\right) + 2\,\mathcal{A}\right]\,(1 \pm \cot\,[\mathrm{x} - \mathcal{G}\,t])^2. \quad (3.27)$$

(1.1.10) Considering the free parameters and their restrictions: The model structure parameters are fixed as $\varrho_0 = \frac{1-m^2}{4}$, $\varrho_2 = \frac{1+m^2}{2}$, $\varrho_4 = \frac{1-m^2}{4}$; the elliptic modulus parameter must satisfy $0 \leq m < 1$ to ensure well-defined periodic solutions; the nonlinear coefficient requires $\rho_5 \neq 0$ to avoid solution singularity; the amplitude parameters $\mathcal{A}$, $\mathfrak{S}$, and $\mathcal{U}$ must satisfy $(2\mathcal{A} + \mathfrak{S})^2 + 40\rho_5\mathcal{U} > 0$ to guarantee real-valued solutions, while the wave velocity $\mathcal{G}$ is a free real parameter ($\mathcal{G} \in \mathbb{R}$), and the sign choice ± generates two distinct solution branches. Under these conditions, the JEF solutions take the following form:

$$\mathfrak{Y}_{1.1.12} = -\frac{3(1-m^2)}{\rho_5}\left[\left(\mathfrak{S} \pm \sqrt{(2\,\mathcal{A} + \mathfrak{S})^2 + 40\,\rho_5\,\mathcal{U}}\right) + 2\,\mathcal{A}\right]\,(\mathrm{nc}\,[\mathrm{x} - \mathcal{G}\,t] \pm \mathrm{sc}\,[\mathrm{x} - \mathcal{G}\,t])^2. \quad (3.28)$$

Setting $m = 0$ in Eq (3.28) yields the singular periodic solution:

$$\mathfrak{Y}_{1.1.12,1} = \frac{3}{\rho_5}\left[\left(\mathfrak{S} \pm \sqrt{(2\,\mathcal{A} + \mathfrak{S})^2 + 40\,\rho_5\,\mathcal{U}}\right) + 2\,\mathcal{A}\right]\,(\sec\,[\mathrm{x} - \mathcal{G}\,t] \pm \tan\,[\mathrm{x} - \mathcal{G}\,t])^2. \quad (3.29)$$

(1.1.11) Considering the free parameters and their restrictions: The model structure parameters are fixed as $\varrho_0 = \frac{m^2}{4}$, $\varrho_2 = \frac{m^2-2}{2}$, $\varrho_4 = \frac{1}{4}$; the elliptic modulus parameter must satisfy $0 \leq m < 1$ to ensure well-defined periodic solutions; the nonlinear coefficient requires $\rho_5 \neq 0$ to avoid solution singularity; the amplitude parameters $\mathcal{A}$, $\mathfrak{S}$, and $\mathcal{U}$ must satisfy $(2\,\mathcal{A} + \mathfrak{S})^2 + 40\,\rho_5\,\mathcal{U} > 0$ to guarantee real-valued solutions, while the wave velocity $\mathcal{G}$ is a free real parameter ($\mathcal{G} \in \mathbb{R}$), and the sign choice ± generates two distinct solution branches. Under these conditions, the JEF solutions take the following form:

$$\mathfrak{Y}_{1.1.13} = -\frac{3(1-m^2)}{\rho_5}\left[\left(\mathfrak{S} \pm \sqrt{(2\,\mathcal{A} + \mathfrak{S})^2 + 40\,\rho_5\,\mathcal{U}}\right) + 2\,\mathcal{A}\right]\,(\mathrm{ns}\,[\mathrm{x} - \mathcal{G}\,t] \pm \mathrm{ds}\,[\mathrm{x} - \mathcal{G}\,t])^2. \quad (3.30)$$

From the previously derived solution set (1.2), we derive exact solutions to Eq (1.1) having the following general form:

(1.2.1) Considering the free parameters and their restrictions: The model structure parameters are fixed as $\varrho_0 = 1$, $\varrho_2 = -m^2 - 1$, $\varrho_4 = m^2$; the elliptic modulus parameter must satisfy $0 \leq m \leq 1$ to ensure well-defined periodic solutions; the nonlinear coefficient requires $\rho_5 \neq 0$ to avoid solution singularity; the amplitude parameters $\mathcal{A}$, $\mathfrak{S}$, and $\mathcal{U}$ must satisfy $(2\,\mathcal{A} + \mathfrak{S})^2 + 40\,\rho_5\,\mathcal{U} > 0$ to guarantee real-valued solutions, while the wave velocity $\mathcal{G}$ is a free real parameter ($\mathcal{G} \in \mathbb{R}$), and the sign choice ± generates two distinct solution branches. Under these conditions, the JEF solutions take the following form:

$$\mathfrak{Y}_{1.2.1} = \frac{3}{\rho_5}\left[\left(\mathfrak{S} \pm \sqrt{(2\,\mathcal{A} + \mathfrak{S})^2 + 40\,\rho_5\,\mathcal{U}}\right) + 2\,\mathcal{A}\right]\,\mathrm{ns}^2\left[\mathrm{x} - \mathcal{G}\,t\right], \tag{3.31}$$

or

$$\mathfrak{Y}_{1.2.2} = \frac{3}{\rho_5}\left[\left(\mathfrak{S} \pm \sqrt{(2\,\mathcal{A} + \mathfrak{S})^2 + 40\,\rho_5\,\mathcal{U}}\right) + 2\,\mathcal{A}\right]\,\mathrm{dc}^2\left[\mathrm{x} - \mathcal{G}\,t\right]. \tag{3.32}$$

Setting$m = 1$ in Eq (3.31) yields the singular soliton solution:

$$\mathfrak{Y}_{1.2.1,1} = -\frac{3}{\rho_5}\left[\left(\mathfrak{S} \pm \sqrt{(2\,\mathcal{A} + \mathfrak{S})^2 + 40\,\rho_5\,\mathcal{U}}\right) + 2\,\mathcal{A}\right]\,\coth^2\left[\mathrm{x} - \mathcal{G}\,t\right]. \tag{3.33}$$

Setting $m = 0$ in Eqs (3.31) and (3.32) yields the singular soliton solution:

$$\mathfrak{Y}_{1.2.1,2} = \frac{3}{\rho_5}\left[\left(\mathfrak{S} \pm \sqrt{(2\,\mathcal{A} + \mathfrak{S})^2 + 40\,\rho_5\,\mathcal{U}}\right) + 2\,\mathcal{A}\right]\,\csc^2\left[\mathrm{x} - \mathcal{G}\,t\right], \tag{3.34}$$

or

$$\mathfrak{Y}_{1.2.2,2} = \frac{3}{\rho_5}\left[\left(\mathfrak{S} \pm \sqrt{(2\,\mathcal{A} + \mathfrak{S})^2 + 40\,\rho_5\,\mathcal{U}}\right) + 2\,\mathcal{A}\right]\,\sec^2\left[\mathrm{x} - \mathcal{G}\,t\right]. \tag{3.35}$$

(1.2.2) Considering the free parameters and their restrictions: The model structure parameters are fixed as $\varrho_0 = 1 - m^2$, $\varrho_2 = m^2 - 1$, $\varrho_4 = -m^2$, the elliptic modulus parameter must satisfy $0 \leq m < 1$ to ensure well-defined periodic solutions; the nonlinear coefficient requires $\rho_5 \neq 0$ to avoid solution singularity; the amplitude parameters $\mathcal{A}$, $\mathfrak{S}$, and $\mathcal{U}$ must satisfy $(2\mathcal{A} + \mathfrak{S})^2 + 40\rho_5\mathcal{U} > 0$ to guarantee real-valued solutions, while the wave velocity $\mathcal{G}$ is a free real parameter ($\mathcal{G} \in \mathbb{R}$), and the sign choice ± generates two distinct solution branches. Under these conditions, the JEF solutions take the following form:

$$\mathfrak{Y}_{1.2.3} = \frac{3\,(1 - m^2)}{\rho_5}\left[\mathfrak{S} + 2\,\mathcal{A} \pm \sqrt{(2\,\mathcal{A} + \mathfrak{S})^2 + 40\,\rho_5\,\mathcal{U}}\right]\,\mathrm{nc}^2\left[\mathrm{x} - \mathcal{G}\,t\right]. \tag{3.36}$$

Setting $m = 0$ in Eq (3.36) yields the singular periodic solution:

$$\mathfrak{Y}_{1.2.3,1} = -\frac{3}{\rho_5}\left[\left(\mathfrak{S} \pm \sqrt{(2\,\mathcal{A} + \mathfrak{S})^2 + 40\,\rho_5\,\mathcal{U}}\right) + 2\,\mathcal{A}\right]\,\sec^2\left[\mathrm{x} - \mathcal{G}\,t\right]. \tag{3.37}$$

(1.2.3) Considering the free parameters and their restrictions: The model structure parameters are fixed as $\varrho_0 = m^2$, $\varrho_2 = -(m^2 + 1)$, $\varrho_4 = 1$; the elliptic modulus parameter must satisfy $0 \leq m \leq 1$ to

ensure well-defined periodic solutions; the nonlinear coefficient requires $\rho_5 \neq 0$ to avoid solution singularity; the amplitude parameters $\mathcal{A}$, $\mathfrak{S}$, and $\mathcal{U}$ must satisfy $(2\,\mathcal{A} + \mathfrak{S})^2 + 40\,\rho_5\,\mathcal{U} > 0$ to guarantee real-valued solutions, while the wave velocity $\mathcal{G}$ is a free real parameter ($\mathcal{G} \in \mathbb{R}$), and the sign choice $\pm$ generates two distinct solution branches. Under these conditions, the JEF solutions take the following form:

$$\mathfrak{Y}_{1.2.4} = -\frac{3}{\rho_5}\left[\left(\mathfrak{S} \pm \sqrt{(2\,\mathcal{A} + \mathfrak{S})^2 + 40\,\rho_5\,\mathcal{U}}\right) + 2\,\mathcal{A}\right]\,\mathrm{sn}^2\left[\mathrm{x} - \mathcal{G}\,t\right], \tag{3.38}$$

or

$$\mathfrak{Y}_{1.2.5} = -\frac{3\,m^2}{\rho_5}\left[\left(\mathfrak{S} \pm \sqrt{(2\,\mathcal{A} + \mathfrak{S})^2 + 40\,\rho_5\,\mathcal{U}}\right) + 2\,\mathcal{A}\right]\,\mathrm{cd}^2\left[\mathrm{x} - \mathcal{G}\,t\right]. \tag{3.39}$$

Setting $m = 1$ in Eq (3.38) yields the dark soliton solution:

$$\mathfrak{Y}_{1.2.4,1} = \frac{3}{\rho_5}\left[\left(\mathfrak{S} \pm \sqrt{(2\,\mathcal{A} + \mathfrak{S})^2 + 40\,\rho_5\,\mathcal{U}}\right) + 2\,\mathcal{A}\right]\,\tanh^2\left[\mathrm{x} - \mathcal{G}\,t\right]. \tag{3.40}$$

(1.2.4) Considering the free parameters and their restrictions: The model structure parameters are fixed as $\varrho_0 = -m^2$, $\varrho_2 = 2m^2 - 1$, $\varrho_4 = 1 - m^2$; the elliptic modulus parameter must satisfy $0 < m \leq 1$ to ensure well-defined periodic solutions; the nonlinear coefficient requires $\rho_5 \neq 0$ to avoid solution singularity; the amplitude parameters $\mathcal{A}$, $\mathfrak{S}$, and $\mathcal{U}$ must satisfy $(2\mathcal{A} + \mathfrak{S})^2 + 40\,\rho_5\,\mathcal{U} > 0$ to guarantee real-valued solutions, while the wave velocity $\mathcal{G}$ is a free real parameter ($\mathcal{G} \in \mathbb{R}$), and the sign choice $\pm$ generates two distinct solution branches. Under these conditions, the JEF solutions take the following form:

$$\mathfrak{Y}_{1.2.5} = -\frac{3\,m^2}{\rho_5}\left[\left(\mathfrak{S} \pm \sqrt{(2\,\mathcal{A} + \mathfrak{S})^2 + 40\,\rho_5\,\mathcal{U}}\right) + 2\,\mathcal{A}\right]\,\mathrm{nc}^2\left[\mathrm{x} - \mathcal{G}\,t\right]. \tag{3.41}$$

Setting $m = 1$ in Eq (3.41) yields the bright soliton solution:

$$\mathfrak{Y}_{1.2.5,1} = \frac{3}{\rho_5}\left[\left(\mathfrak{S} \pm \sqrt{(2\,\mathcal{A} + \mathfrak{S})^2 + 40\,\rho_5\,\mathcal{U}}\right) + 2\,\mathcal{A}\right]\,\mathrm{sech}^2\left[\mathrm{x} - \mathcal{G}\,t\right]. \tag{3.42}$$

(1.2.5) Considering the free parameters and their restrictions: The model structure parameters are fixed as $\varrho_0 = 1$, $\varrho_2 = 2 - m^2$, $\varrho_4 = 1 - m^2$; the elliptic modulus parameter must satisfy $0 \leq m \leq 1$ to ensure well-defined periodic solutions; the nonlinear coefficient requires $\rho_5 \neq 0$ to avoid solution singularity; the amplitude parameters $\mathcal{A}$, $\mathfrak{S}$, and $\mathcal{U}$ must satisfy $(2\mathcal{A} + \mathfrak{S})^2 + 40\,\rho_5\,\mathcal{U} > 0$ to guarantee real-valued solutions, while the wave velocity $\mathcal{G}$ is a free real parameter ($\mathcal{G} \in \mathbb{R}$), and the sign choice $\pm$ generates two distinct solution branches. Under these conditions, the JEF solutions take the following form:

$$\mathfrak{Y}_{1.2.6} = \frac{3}{\rho_5}\left[\left(\mathfrak{S} \pm \sqrt{(2\,\mathcal{A} + \mathfrak{S})^2 + 40\,\rho_5\,\mathcal{U}}\right) + 2\,\mathcal{A}\right]\,\mathrm{cs}^2\left[\mathrm{x} - \mathcal{G}\,t\right]. \tag{3.43}$$

Setting $m = 1$ or $m = 0$ in Eq (3.43) yields the singular soliton solution or singular periodic solution:

$$\mathfrak{Y}_{1.2.6,1} = \frac{3}{\rho_5}\left[\left(\mathfrak{S} \pm \sqrt{(2\,\mathcal{A} + \mathfrak{S})^2 + 40\,\rho_5\,\mathcal{U}}\right) + 2\,\mathcal{A}\right]\mathrm{csch}^2\left[\mathrm{x} - \mathcal{G}\,t\right], \tag{3.44}$$

or

$$\mathfrak{Y}_{1.2.6,2} = \frac{3}{\rho_5}\left[\left(\mathfrak{S} \pm \sqrt{(2\,\mathcal{A} + \mathfrak{S})^2 + 40\,\rho_5\,\mathcal{U}}\right) + 2\,\mathcal{A}\right]\cot^2\left[\mathrm{x} - \mathcal{G}\,t\right]. \tag{3.45}$$

(1.2.6) Considering the free parameters and their restrictions: The model structure parameters are fixed as $\varrho_0 = 1$, $\varrho_2 = 2m^2 - 1$, $\varrho_4 = -m^2(1 - m^2)$; the elliptic modulus parameter must satisfy $0 \leq m \leq 1$ to ensure well-defined periodic solutions; the nonlinear coefficient requires $\rho_5 \neq 0$ to avoid solution singularity; the amplitude parameters $\mathcal{A}$, $\mathfrak{S}$, and $\mathcal{U}$ must satisfy $(2\mathcal{A} + \mathfrak{S})^2 + 40\rho_5\mathcal{U} > 0$ to guarantee real-valued solutions, while the wave velocity $\mathcal{G}$ is a free real parameter ($\mathcal{G} \in \mathbb{R}$), and the sign choice ± generates two distinct solution branches. Under these conditions, the JEF solutions take the following form:

$$\mathfrak{Y}_{1.2.7} = \frac{3}{\rho_5}\left[\left(\mathfrak{S} \pm \sqrt{(2\,\mathcal{A} + \mathfrak{S})^2 + 40\,\rho_5\,\mathcal{U}}\right) + 2\,\mathcal{A}\right]\,\mathrm{ds}^2\left[\mathrm{x} - \mathcal{G}\,t\right]. \tag{3.46}$$

Setting $m = 1$ or $m = 0$ in Eq (3.46) yields the singular soliton solution or singular periodic solution:

$$\mathfrak{Y}_{1.2.7,1} = \frac{3}{\rho_5}\left[\left(\mathfrak{S} \pm \sqrt{(2\,\mathcal{A} + \mathfrak{S})^2 + 40\,\rho_5\,\mathcal{U}}\right) + 2\,\mathcal{A}\right]\mathrm{csch}^2\left[\mathrm{x} - \mathcal{G}\,t\right], \tag{3.47}$$

or

$$\mathfrak{Y}_{1.2.7,2} = \frac{3}{\rho_5}\left[\left(\mathfrak{S} \pm \sqrt{(2\,\mathcal{A} + \mathfrak{S})^2 + 40\,\rho_5\,\mathcal{U}}\right) + 2\,\mathcal{A}\right]\mathrm{csc}^2\left[\mathrm{x} - \mathcal{G}\,t\right]. \tag{3.48}$$

(1.2.7) Considering the free parameters and their restrictions: The model structure parameters are fixed as $\varrho_0 = 1 - m^2$, $\varrho_2 = 2 - m^2$, $\varrho_4 = 1$; the elliptic modulus parameter must satisfy $0 \leq m < 1$ to ensure well-defined periodic solutions; the nonlinear coefficient requires $\rho_5 \neq 0$ to avoid solution singularity; the amplitude parameters $\mathcal{A}$, $\mathfrak{S}$, and $\mathcal{U}$ must satisfy $(2\,\mathcal{A} + \mathfrak{S})^2 + 40\,\rho_5\,\mathcal{U} > 0$ to guarantee real-valued solutions, while the wave velocity $\mathcal{G}$ is a free real parameter ($\mathcal{G} \in \mathbb{R}$), and the sign choice ± generates two distinct solution branches. Under these conditions, the JEF solutions take the following form:

$$\mathfrak{Y}_{1.2.8} = \frac{3\,(m^2 - 1)}{\rho_5}\left[\left(\mathfrak{S} \pm \sqrt{(2\,\mathcal{A} + \mathfrak{S})^2 + 40\,\rho_5\,\mathcal{U}}\right) + 2\,\mathcal{A}\right]\,\mathrm{sc}^2\left[\mathrm{x} - \mathcal{G}\,t\right]. \tag{3.49}$$

Setting $m = 0$ in Eq (3.49) yields the singular periodic solution:

$$\mathfrak{Y}_{1.2.8,1} = \frac{3}{\rho_5}\left[\left(\mathfrak{S} \pm \sqrt{(2\,\mathcal{A} + \mathfrak{S})^2 + 40\,\rho_5\,\mathcal{U}}\right) + 2\,\mathcal{A}\right]\tan^2\left[\mathrm{x} - \mathcal{G}\,t\right]. \tag{3.50}$$

(1.2.8) Considering the free parameters and their restrictions: The model structure parameters are fixed as $\varrho_0 = \frac{1}{4}$, $\varrho_2 = \frac{1-2m^2}{2}$, $\varrho_4 = \frac{1}{4}$; the elliptic modulus parameter must satisfy $0 \leq m \leq 1$ to ensure well-defined periodic solutions; the nonlinear coefficient requires $\rho_5 \neq 0$ to avoid solution singularity; the amplitude parameters $\mathcal{A}$, $\mathfrak{S}$, and $\mathcal{U}$ must satisfy $(2\mathcal{A} + \mathfrak{S})^2 + 40\rho_5\mathcal{U} > 0$ to guarantee real-valued solutions, while the wave velocity $\mathcal{G}$ is a free real parameter ($\mathcal{G} \in \mathbb{R}$), and the sign choice ± generates two distinct solution branches. Under these conditions, the JEF solutions take the following form:

$$\mathfrak{Y}_{1.1.9} = \frac{3\left((2\mathcal{A} + \mathfrak{S}) \pm \sqrt{(2\mathcal{A} + \mathfrak{S})^2 + 40\rho_5\mathcal{U}}\right)}{4\,\rho_5\,(\mathrm{cs}\left[\mathrm{x} - \mathcal{G}\,t\right] \pm \mathrm{nd}\left[\mathrm{x} - \mathcal{G}\,t\right])^2}. \tag{3.51}$$

Setting $m = 1$ or $m = 0$ in Eq (3.51) yields the hyperbolic solution, or singular periodic solution:

$$\mathfrak{Y}_{1.2.9,1} = \frac{3\left((2\mathcal{A} + \mathfrak{S}) \pm \sqrt{(2\mathcal{A} + \mathfrak{S})^2 + 40\rho_5\mathcal{U}}\right)}{4\rho_5(\cosh[\mathrm{x} - \mathcal{G}\,t] \pm \mathrm{csch}[\mathrm{x} - \mathcal{G}\,t])^2}, \tag{3.52}$$

or

$$\mathfrak{Y}_{1.2.9,2} = \frac{3\left(2\mathcal{A} + \mathfrak{S} \pm \sqrt{(2\mathcal{A} + \mathfrak{S})^2 + 40\rho_5\mathcal{U}}\right)}{4\,\rho_5(1 \pm \cot[\mathrm{x} - \mathcal{G}\,t])^2}. \tag{3.53}$$

(1.2.10) Considering the free parameters and their restrictions: The model structure parameters are fixed as $\varrho_0 = \frac{1-m^2}{4}$, $\varrho_2 = \frac{1+m^2}{2}$, $\varrho_4 = \frac{1-m^2}{4}$; the elliptic modulus parameter must satisfy $0 \leq m < 1$ to ensure well-defined periodic solutions; the nonlinear coefficient requires $\rho_5 \neq 0$ to avoid solution singularity; the amplitude parameters $\mathcal{A}$, $\mathfrak{S}$, and $\mathcal{U}$ must satisfy $(2\mathcal{A} + \mathfrak{S})^2 + 40\rho_5\mathcal{U} > 0$ to guarantee real-valued solutions, while the wave velocity $\mathcal{G}$ is a free real parameter ($\mathcal{G} \in \mathbb{R}$), and the sign choice $\pm$ generates two distinct solution branches. Under these conditions, the JEF solutions take the following form:

$$\mathfrak{Y}_{1.2.10} = -\frac{3\left(m^2 - 1\right)\left(2\mathcal{A} + \mathfrak{S} \pm \sqrt{(2\mathcal{A} + \mathfrak{S})^2 + 40\rho_5\mathcal{U}}\right)}{4\,\rho_5\,(\mathrm{nc}[\mathrm{x} - \mathcal{G}\,t] \pm \mathrm{sc}[\mathrm{x} - \mathcal{G}\,t])^2}. \tag{3.54}$$

Setting $m = 0$ in Eq (3.54) yields the singular periodic solution:

$$\mathfrak{Y}_{1.2.10,1} = \frac{3\left(2\mathcal{A} + \mathfrak{S} \pm \sqrt{(2\mathcal{A} + \mathfrak{S})^2 + 40\rho_5\mathcal{U}}\right)}{4\rho_5(\sec[\mathrm{x} - \mathcal{G}\,t] \pm \tan[\mathrm{x} - \mathcal{G}\,t])^2}. \tag{3.55}$$

(1.2.11) Considering the free parameters and their restrictions: The model structure parameters are fixed as $\varrho_0 = \frac{m^2}{4}$, $\varrho_2 = \frac{m^2-2}{2}$, $\varrho_4 = \frac{1}{4}$; the elliptic modulus parameter must satisfy $0 < m \leq 1$ to ensure well-defined periodic solutions; the nonlinear coefficient requires $\rho_5 \neq 0$ to avoid solution singularity; the amplitude parameters $\mathcal{A}$, $\mathfrak{S}$, and $\mathcal{U}$ must satisfy $(2\mathcal{A} + \mathfrak{S})^2 + 40\rho_5\mathcal{U} > 0$ to guarantee real-valued solutions, while the wave velocity $\mathcal{G}$ is a free real parameter ($\mathcal{G} \in \mathbb{R}$), and the sign choice $\pm$ generates two distinct solution branches. Under these conditions, the JEF solutions take the following form:

$$\mathfrak{Y}_{1.2.11} = \frac{3\,m^2\left(2\mathcal{A} + \mathfrak{S} \pm \sqrt{(2\mathcal{A} + \mathfrak{S})^2 + 40\rho_5\mathcal{U}}\right)}{4\rho_5(\mathrm{ns}[\mathrm{x} - \mathcal{G}\,t] \pm \mathrm{ds}[\mathrm{x} - \mathcal{G}\,t])^2}. \tag{3.56}$$

Setting $m = 1$ in Eq (3.56) yields the singular soliton solution or singular soliton solution:

$$\mathfrak{Y}_{1.2.11,1} = \frac{3\left((2\mathcal{A} + \mathfrak{S}) \pm \sqrt{(2\mathcal{A} + \mathfrak{S})^2 + 40\rho_5\mathcal{U}}\right)}{4\rho_5(\coth[\mathrm{x} - \mathcal{G}\,t] \pm \mathrm{csch}[\mathrm{x} - \mathcal{G}\,t])^2}. \tag{3.57}$$

Second case. Under the constraints $\varrho_0 = \varrho_1 = 0$, the algebraic system undergoes a fundamental transformation, resulting in a solution space defined by:

$$\beta_2 = 0, \quad \alpha_2 = \frac{3\,\varrho_4\left(2\,\mathcal{A}+\mathfrak{S}+\sqrt{((2\,\mathcal{A}+\mathfrak{S})^2+40\,\rho_5\,\mathcal{U})}\right)}{\rho_5}, \quad \rho_4 = \frac{\varrho_2\,(4\,\mathcal{G}\,\rho_3-4\,\rho_2+16\,\mathcal{U}\,\varrho_2)+\mathcal{G}}{4\,\mathcal{G}^2\,\varrho_2}, \quad \varrho_3 = 0,$$
$$\mathcal{V} = \frac{\mathcal{L}\left(2\,\mathcal{A}+\mathfrak{S}-\sqrt{(2\,\mathcal{A}+\mathfrak{S})^2+40\rho_5\mathcal{U}}\right)}{2\mathcal{U}}, \; \mathcal{J} = 0, \; \rho_1 = \frac{1}{40\,\mathcal{U}\,\varrho_2}\,[\left(64\,\mathcal{U}\,\varrho_2^2 - \mathcal{G}\right)\sqrt{(2\,\mathcal{A}+\mathfrak{S})^2+40\,\rho_5\,\mathcal{U}} +$$
$$\mathcal{G}(2\,\mathcal{A}+\mathfrak{S}) + 8\,\mathcal{U}\,\varrho_2\,(4\,\varrho_2\,(\mathcal{A}+20\,\mathcal{L}\,\varrho_2+3\,\mathfrak{S})+5\,\mathfrak{T})].$$

From the previously derived solution set, we derive exact solutions to Eq (1.1) having the following general form:
Under the conditions $\rho_5 \neq 0$, $(2\mathcal{A} + \mathfrak{S})^2 + 40\rho_5\,\mathcal{U} > 0$, $\varrho_2 > 0$, $\varrho_3 = 0$, and $\epsilon = \pm 1$, exponential solution takes the following form:

$$\mathfrak{Y}_2 = \frac{48\,\varrho_2^2\,\varrho_4\,\sqrt{(2\mathcal{A}+\mathfrak{S})^2 + 40\,\rho_5\,\mathcal{U}} + 2\,\mathcal{A} + \mathfrak{S} e^{[2\,\epsilon(\mathrm{x}-\mathcal{G}\,t)\,\sqrt{\varrho_2}]}}{\rho_5\,\left(1 - 4\,\varrho_2\,\varrho_4\,e^{[2\,\epsilon\,(\mathrm{x}-\mathcal{G}\,t)\,\sqrt{\varrho_2}]}\right)^2}. \tag{3.58}$$

Third case. Under the constraints $\varrho_0 = \varrho_1 = \varrho_3 = 0$, the algebraic system undergoes a fundamental transformation, resulting in a solution space defined by:

$$\beta_2 = 0, \alpha_2 = \frac{3\varrho_4[(2\mathcal{A}+\mathfrak{S})\pm 3\sqrt{((2\mathcal{A}+\mathfrak{S})^2+40\rho_5\mathcal{U})}]}{\rho_5},\ \rho_4 = \frac{\varrho_2(4\mathcal{G}\rho_3 - 4\rho_2 + 16\mathcal{U}\varrho_2)+\mathcal{G}}{4\mathcal{G}^2\varrho_2},\ \mathcal{J} = 0,\ \mathcal{V} = \frac{1}{2\mathcal{U}\varrho_4}(\mathcal{L}[\varrho_4(2\mathcal{A} + \mathfrak{S}) \mp \sqrt{\varrho_4^2\,((2\,\mathcal{A}+\mathfrak{S})^2 + 40\,\rho_5\mathcal{U})}]),\ \rho_1 = \frac{1}{40\,\mathcal{U}\,\varrho_2\,\varrho_4}(\varrho_4\,(\mathcal{G}\,(2\,\mathcal{A}+\mathfrak{S}) + 8\,\mathcal{U}\,\varrho_2\,(4\varrho_2\,(\mathcal{A}+20\,\mathcal{L}\,\varrho_2 + 3\,\mathfrak{S}) + 5\,\mathfrak{T})) \pm (\mathcal{G} - 64\,\mathcal{U}\,\varrho_2^2)\sqrt{\varrho_4^2((2\,\mathcal{A}+\mathfrak{S})^2 + 40\,\rho_5\,\mathcal{U})}).$$

From the previously derived solution set, we derive exact solutions to Eq (1.1) having the following general form:

(3.1) Considering the free parameters and their restrictions: The parameter ϱ_2 must be positive ($\varrho_2 > 0$) to ensure the soliton's argument is real the nonlinear coefficient ρ_5 must be nonzero ($\rho_5 \neq 0$) to avoid solution singularity; the parameter ϱ_4 must be negative ($\varrho_4 < 0$) for the existence of the bright soliton; the amplitude parameters $\mathcal{A}$, $\mathfrak{S}$, and $\mathcal{U}$ must satisfy $(2\mathcal{A} + \mathfrak{S})^2 + 40\rho_5\mathcal{U} > 0$ to guarantee real-valued solutions, while the wave velocity $\mathcal{G}$ is a free real parameter ($\mathcal{G} \in \mathbb{R}$), and the sign choice $\pm$ generates two distinct solution branches. Under these conditions, the bright soliton solution takes the following form:

$$\mathfrak{Y}_{3.1} = -\frac{3\,\varrho_2}{\rho_5}\,[\mathfrak{S} + 2\mathcal{A} \pm \sqrt{(2\mathcal{A}+\mathfrak{S})^2 + 40\,\rho_5\,\mathcal{U}}]\,\operatorname{sech}^2\left[(\mathrm{x} - \mathcal{G}\,t)\,\sqrt{\varrho_2}\right]. \tag{3.59}$$

(3.2) Considering the free parameters and their restrictions: The parameter ϱ_2 must be zero ($\varrho_2 = 0$) for this rational solution; the nonlinear coefficient ρ_5 must be nonzero ($\rho_5 \neq 0$) to avoid solution singularity; the parameter ϱ_4 must be positive ($\varrho_4 > 0$) for the existence of this rational wave solution; the amplitude parameters $\mathcal{A}$, $\mathfrak{S}$, and $\mathcal{U}$ must satisfy $(2\mathcal{A}+\mathfrak{S})^2 + 40\rho_5\mathcal{U} > 0$ to guarantee real-valued solutions, while the wave velocity $\mathcal{G}$ is a free real parameter ($\mathcal{G} \in \mathbb{R}$). Under these conditions, the rational solution takes the following form:

$$\mathfrak{Y}_{3.2} = \frac{3\left[(2\,\mathcal{A}+\mathfrak{S}) \pm \sqrt{(2\,\mathcal{A}+\mathfrak{S})^2 + 40\,\rho_5\,\mathcal{U}}\right]}{\rho_5\,(\mathrm{x} - \mathcal{G}\,t)^2}. \tag{3.60}$$

4. Stability analysis for the proposed equation

The analysis of nonlinear wave equations and their stability lies at the heart of modern mathematical physics, with profound implications in diverse fields such as fluid dynamics, optics, plasma physics, and condensed matter systems. These equations describe the dynamics of coherent

structures—including solitons, rogue waves, and dispersive shock waves—whose stability critically influences their observable behavior in both natural phenomena and technological applications.

To examine the linear stability of the system, we introduce small-amplitude perturbations over a homogeneous background solution $\mathcal{Q}$. This approach adheres to the conventional framework for studying modulation instability in nonlinear wave systems [33].

The perturbed solution is expressed in the form:

$$\mathfrak{Y}(\mathrm{x}, t) = \mathcal{P}\,\mathcal{H}(\mathrm{x}, t) + \mathcal{Q}, \tag{4.1}$$

where $\mathcal{Q}$ is the constant background, $\mathcal{H}$ is the perturbation amplitude, and $\mathcal{P}$ is the nonlinearity coefficient governing the system's response.

For any given m, the linearization procedure gives:

$$-[\mathcal{P}\,\mathcal{Q}\,\mathcal{L} + \mathcal{P}\,\mathcal{U}]\,\mathcal{H}_{\mathrm{xxxxx}} + (\mathcal{P}\,\rho_2 - \mathcal{A}\,\mathcal{P}\,\mathcal{Q})\,\mathcal{H}_{\mathrm{xxx}} + \mathcal{P}\,\rho_3\,\mathcal{H}_{\mathrm{xxt}} + \left(\mathcal{P}\,\mathcal{Q}^2\,\rho_5 + \mathcal{P}\,\mathcal{Q}\,\rho_1 - \mathcal{P}\,\mathcal{Q}\,\mathfrak{T}\right)\,\mathcal{H}_x +$$

$$\mathcal{P}\,\rho_4\,\mathcal{H}_{\mathrm{xtt}} + \mathcal{P}\,\mathcal{H}_t = 0. \tag{4.2}$$

We examine small-amplitude plane wave perturbations expressed as:

$$\mathcal{H} = e^{(\mathcal{J}\,t + i\,\Gamma\,\mathrm{x})}, \tag{4.3}$$

where Γ denotes the wave number and $\mathcal{J}$ represents the dispersion relation, and we derive the dispersion relation:

$$\mathcal{J} = \frac{1}{2\,\Gamma\,\rho_4}[i\left(1 - \Gamma^2\,\rho_3\right) \pm \sqrt{4\,\Gamma^2\,\rho_4\,\left(-\mathcal{A}\,\Gamma^2\,\mathcal{Q} + \Gamma^2\,\rho_2 - \mathcal{Q}\,\left(\mathcal{Q}\rho_5 + \rho_1\right) + \mathcal{Q}\,\mathfrak{T} + \Gamma^4\,\left(\mathcal{U} + \mathcal{Q}\,\mathcal{L}\right)\right) - \left(\Gamma^2\,\rho_3 - 1\right)^2}]. \tag{4.4}$$

The stability characteristics of the system are determined by the real part of the dispersion relation $\mathcal{J}$. When the following conditions are satisfied $4\;\Gamma^2\;\rho_4\;\left(-\mathcal{A}\,\Gamma^2\,\mathcal{Q} + \Gamma^2\,\rho_2 - \mathcal{Q}\,\left(\mathcal{Q}\rho_5 + \rho_1\right) + \mathcal{Q}\,\mathfrak{T} + \Gamma^4\,\left(\mathcal{U} + \mathcal{Q}\,\mathcal{L}\right)\right) - \left(\Gamma^2\,\rho_3 - 1\right)^2 > 0$, and $\Gamma\;\rho_4 \neq 0$, the system is marginally stable when $R(\mathcal{J}) = 0$, the system is unstable when $R(\mathcal{J}) > 0$, and the system is stable when $R(\mathcal{J}) < 0$. When the following conditions are satisfied $4\;\Gamma^2\;\rho_4\;\left(-\mathcal{A}\,\Gamma^2\,\mathcal{Q} + \Gamma^2\,\rho_2 - \mathcal{Q}\,\left(\mathcal{Q}\rho_5 + \rho_1\right) + \mathcal{Q}\,\mathfrak{T} + \Gamma^4\,\left(\mathcal{U} + \mathcal{Q}\,\mathcal{L}\right)\right) - \left(\Gamma^2\,\rho_3 - 1\right)^2 < 0$, and $\Gamma\;\rho_4 \neq 0$, then the system is marginally stable since $R(\mathcal{J}) = 0$. To substantiate our theoretical stability analysis with numerical evidence, we present comprehensive graphical representations in Figure 1. These visualizations provide concrete support for the stability claims derived from the dispersion relation analysis.

The graphical analysis in Figure 1 confirms the theoretical stability predictions derived from Eq (4.4). Figure 1(a) illustrates the complex behavior of the dispersion relation across parameter space, while Figures 1(b),(c) demonstrate the three-dimensional structure of stability regions. Most notably, Figure 1(d) provides clear numerical evidence distinguishing between stable and unstable regimes, with the transition boundaries aligning precisely with our analytical conditions $R(J) = 0$. These visualizations not only validate our theoretical framework but also offer practical insights for parameter selection in experimental implementations.

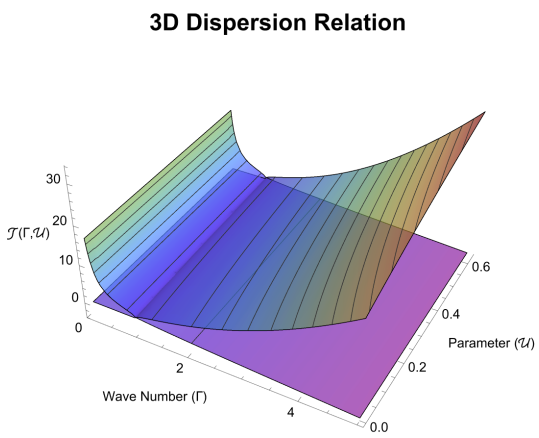

(a) Three-dimensional representation of dispersion relation.

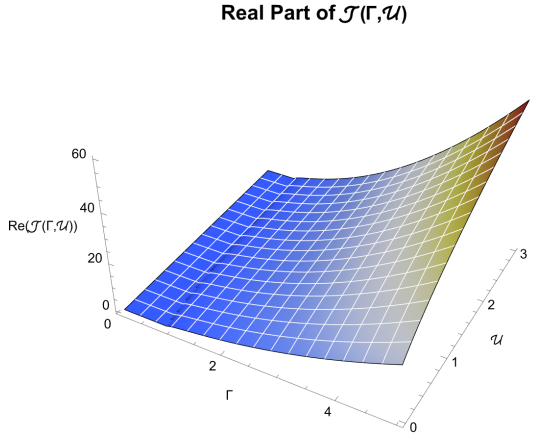

(b) Three-dimensional representation of stability regions.

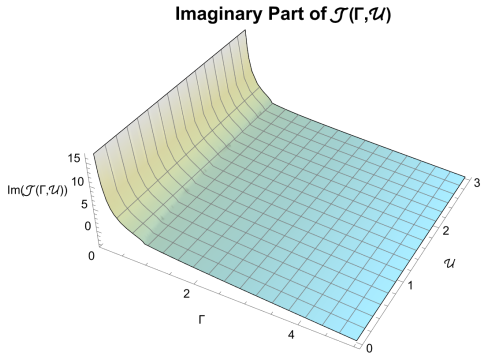

(c) Three-dimensional representation of wave propagation.

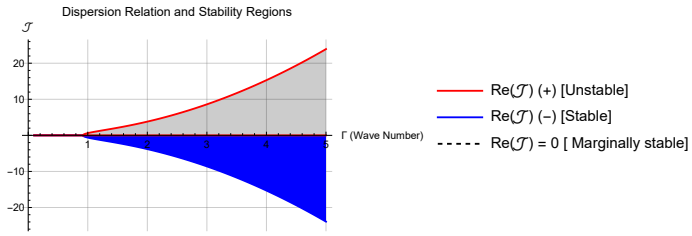

(d) Two-dimensional stability profile.

Figure 1. Numerical validation of stability analysis through comprehensive visualization of the dispersion relation $\mathcal{J}$. Figures 1(a)–(c) provide three-dimensional representations of different aspects of the dispersion characteristics, while Figure 1(d) offers a two-dimensional profile that clearly delineates stable and unstable parameter regions based on the real part of $\mathcal{J}$. These graphical results provide strong numerical evidence supporting our theoretical stability claims.

5. Dynamical behavior of extracted wave solutions

This section examines the diverse exact solutions of the Gardner equation with higher-order dispersion through comprehensive graphical representations and detailed physical analysis, highlighting their unique characteristics and applications in nonlinear wave phenomena. When analyzing the dark soliton from Eq (3.5) with parameters: $\rho_5 = -0.27$, $\mathcal{A} = 2.72$, $\mathfrak{S} = 0.64$, $\mathcal{U} = 0.9$, and $\mathcal{G} = 0.7$, Figure 2 demonstrates a characteristic intensity dip propagating on a continuous background. The visualization clearly shows a stable wave profile with well-defined depth and width parameters, maintaining constant phase shift across the intensity minimum. The dark soliton exhibits remarkable stability against small perturbations, preserving its waveform integrity over extended propagation distances. This behavior is particularly significant for applications in nonlinear optical

systems and Bose-Einstein condensates, where phase-sensitive phenomena are crucial. The bright soliton obtained from Eq (3.7) with parameters $\rho_5 = -0.37$, $\mathcal{A} = 2.12$, $\mathfrak{S} = 0.74$, $\mathcal{U} = 0.9$, and $\mathcal{G} = 0.8$ is visualized in Figure 3. The figure displays a localized, hump-shaped wave packet with symmetric exponential decay on both sides, characteristic of fundamental soliton behavior. The solution maintains constant amplitude and width during propagation, resulting from the precise balance between nonlinear steepening and dispersive spreading effects. This perfect energy localization makes it ideal for optical fiber communications and modeling oceanic internal waves. Figure 4 presents the singular soliton solution from Eq (3.12) with parameters: $\rho_5 = 0.37$, $\mathcal{A} = 0.82$, $\mathfrak{S} = 0.7$, $\mathcal{U} = 0.79$, and $\mathcal{G} = 0.8$. The visualization reveals sharp, cusp-like profiles with intense energy concentration in localized regions, approaching mathematical singularities. This explosive wave behavior manifests in physical contexts such as shock wave formation and plasma wave collapse, where nonlinear self-focusing effects lead to extreme wave amplification and gradient discontinuities. The singular periodic solution from Eq (3.13) with parameters $\rho_5 = 0.47$, $\mathcal{A} = 0.52$, $\mathfrak{S} = 0.57$, $\mathcal{U} = 0.69$, and $\mathcal{G} = 0.58$ is shown in Figure 5. The figure displays a complex wave profile combining periodicity with localized intensity singularities at regular intervals. This hybrid structure captures the essential physics of modulation instability, where periodic background waves develop extreme amplitudes through exponential perturbation growth. Such behavior provides crucial insights for rogue wave prediction in oceanography and voltage surge analysis in electrical systems. The systematic comparison across Figures 2–5 demonstrate the rich solution diversity governed by the perturbed Gardner equation. Each solution type occupies distinct parameter regimes, with the dispersion triplet parameters controlling transitions between dark, bright, singular, and periodic behaviors. The quantitative features extracted from these visualizations—including amplitude profiles, decay characteristics, and singularity patterns—provide experimentalists with precise guidelines for generating specific wave types in laboratory settings and technological applications. The enhanced graphical representations and their detailed descriptions establish clear connections between mathematical solutions and physical manifestations across diverse scientific domains, including nonlinear optics, plasma physics, fluid dynamics, and engineering systems.

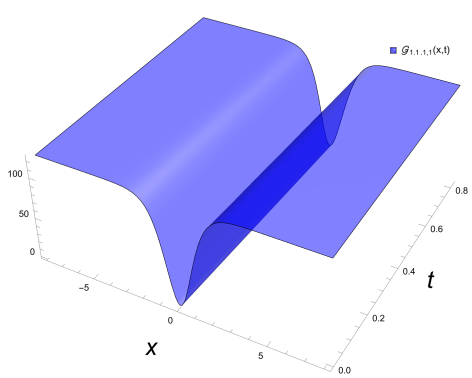

(a) 3D spatiotemporal evolution.

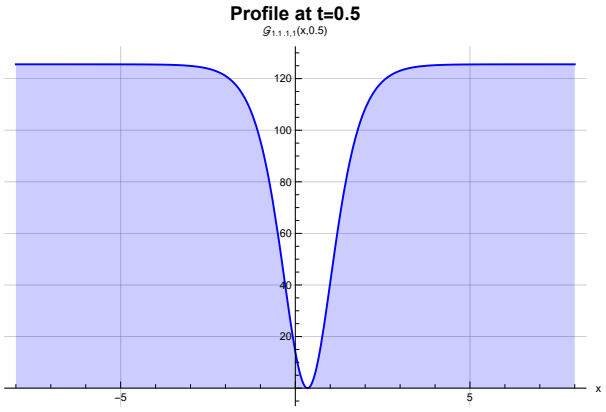

(b) Transverse profile at fixed time.

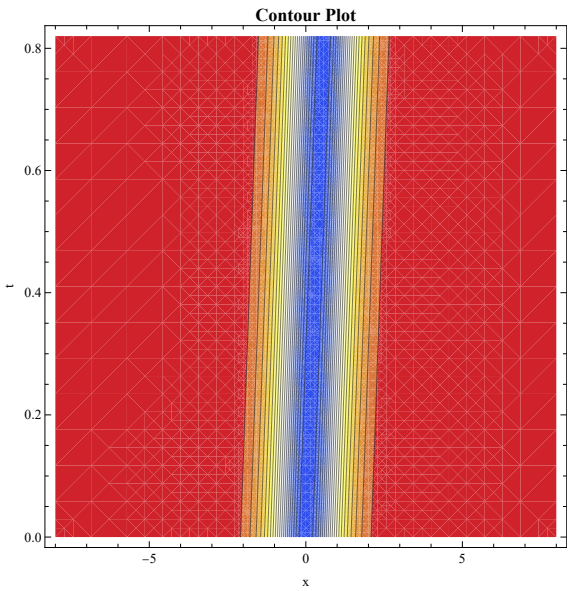

(c) Contour map of intensity distribution.

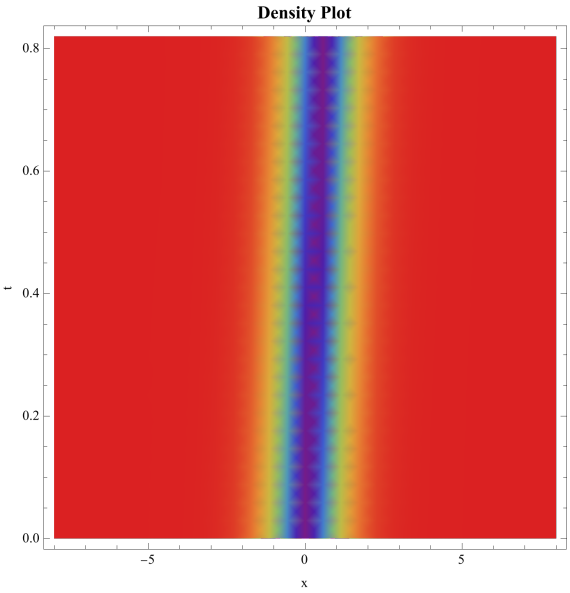

(d) Stability regions classification.

Figure 2. Visualization of dark soliton solution for Eq (3.5).

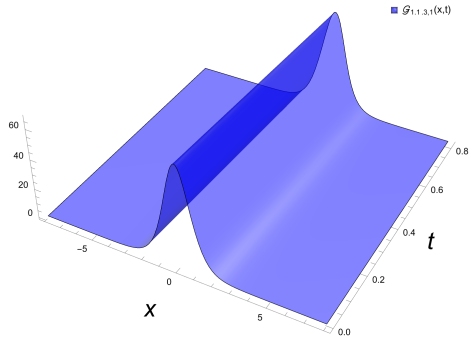

(a) 3D spatiotemporal evolution.

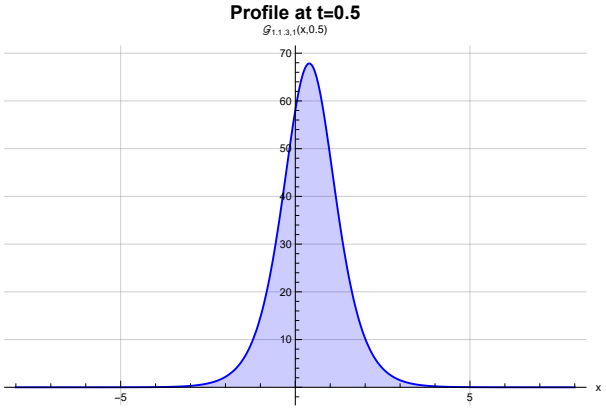

(b) Transverse profile at fixed time.

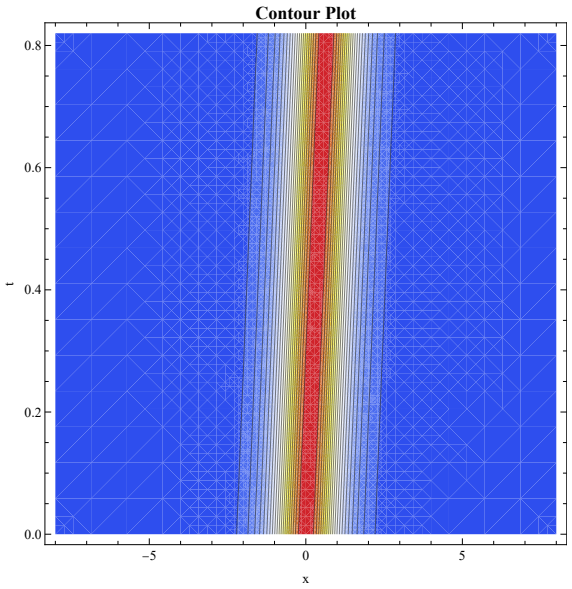

(c) Contour map of intensity distribution.

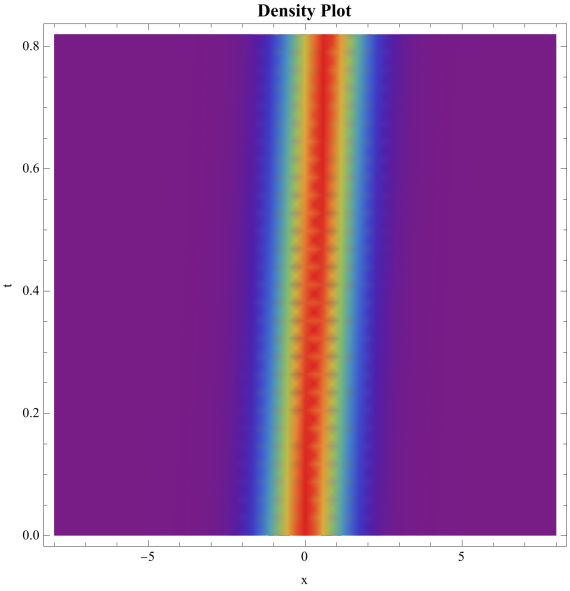

(d) Stability regions classification.

Figure 3. Visualization of bright soliton solution for Eq (3.7).

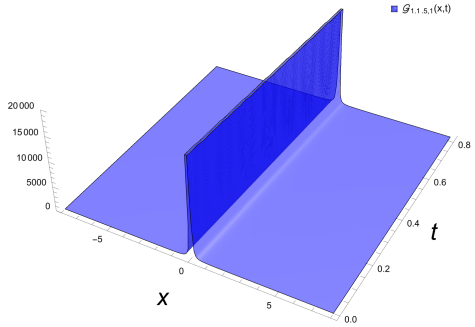

(a) 3D spatiotemporal evolution.

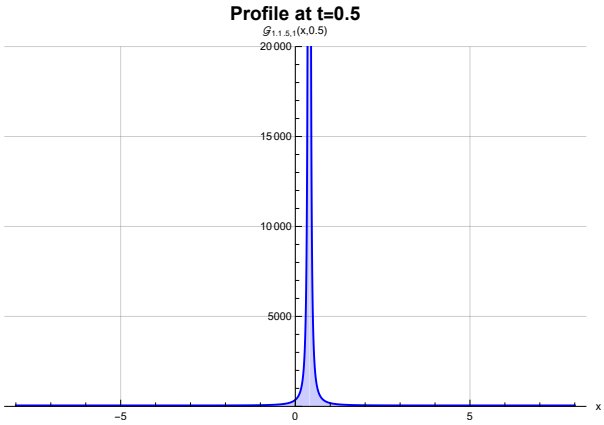

(b) Transverse profile at fixed time.

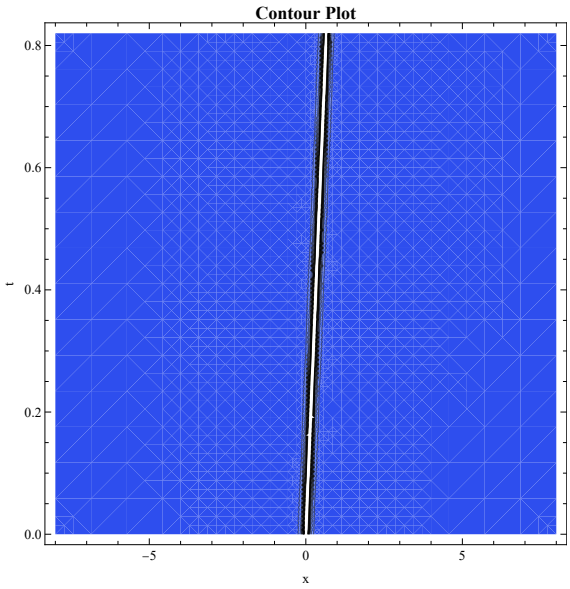

(c) Contour map of intensity distribution.

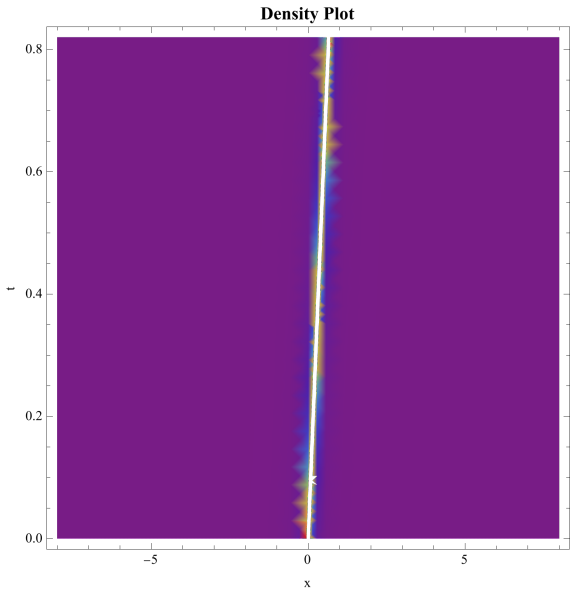

(d) Stability regions classification.

Figure 4. Visualization of singular soliton solution for Eq (3.12).

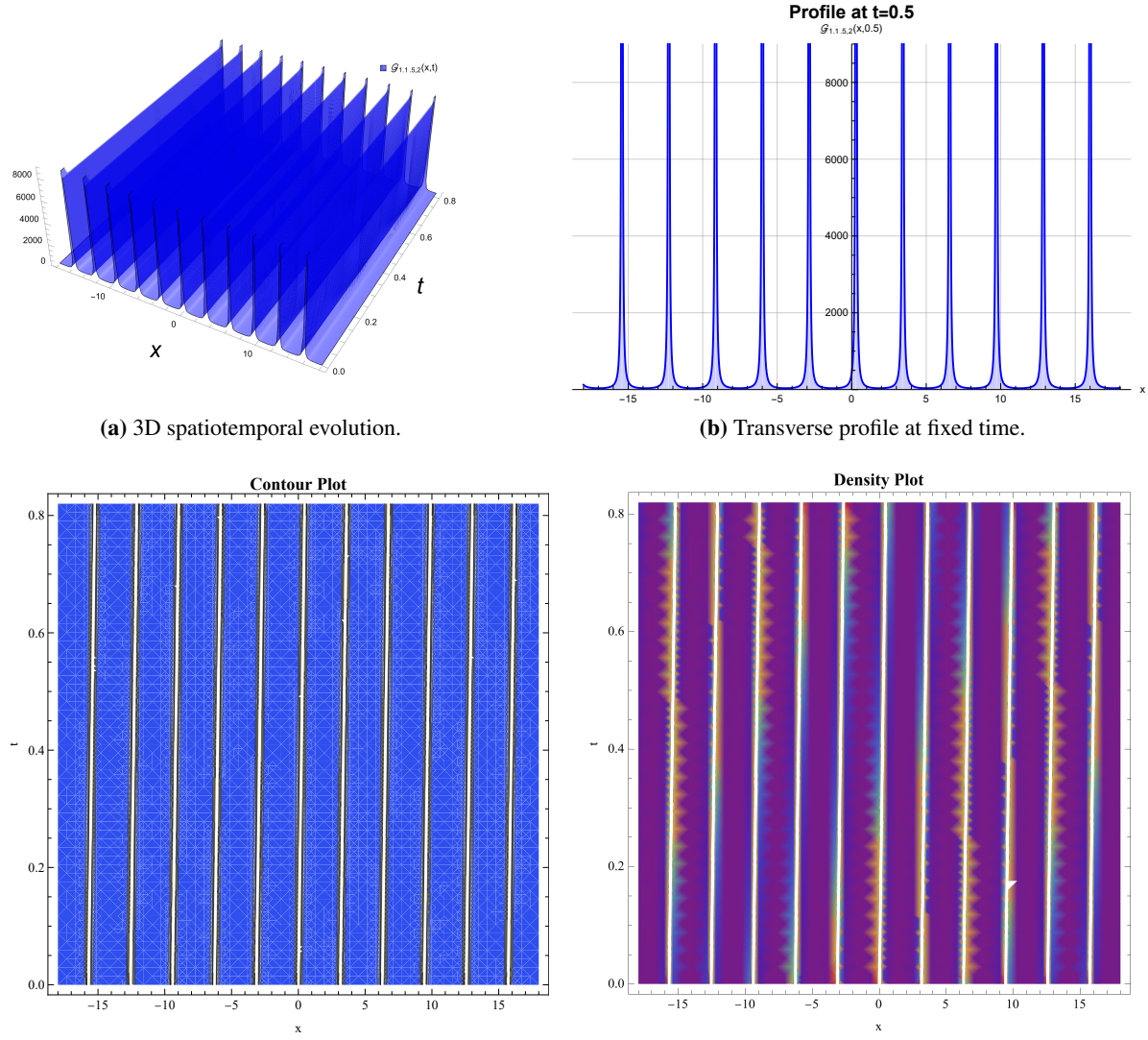

(a) 3D spatiotemporal evolution.

(b) Transverse profile at fixed time.

(c) Contour map of intensity distribution.

(d) Stability regions classification.

Figure 5. Visualization of singular periodic solution for Eq (3.13).

6. Conclusions

This research has established a comprehensive theoretical framework for analyzing the perturbed Gardner equation with higher-order dispersion through the development of an innovative extended F-expansion technique. Our methodology has successfully generated a diverse family of exact analytical solutions, including bright and dark solitons, singular solutions, periodic wave patterns, and rational solutions, while systematically addressing mathematical complexities arising from higher-order nonlinearities and perturbation effects. The inclusion of higher-order dispersion terms fundamentally reshapes wave stability and propagation dynamics, enabling novel solution classes absent in conventional Gardner equation models. These terms introduce additional degrees of freedom that permit fine-tuning of wave characteristics. We have established precise parameter

constraints that guarantee physically meaningful solutions across different wave regimes, ensuring mathematical solutions correspond to observable physical phenomena. The intricate interplay between nonlinearity and dispersion creates distinct stability windows for each solution type, governed by specific energy distribution patterns and phase relationships that determine solution viability. The core findings of our study demonstrate that the higher-order dispersion terms fundamentally alter the stability and propagation characteristics of nonlinear waves, enabling new classes of solutions not observed in standard Gardner equation models, the specific parameter constraints we derived ensure physically meaningful solutions across different wave regimes, and the interaction between nonlinearity and dispersion creates distinct stability windows for each solution type. These findings align with recent advances in nonlinear wave theory, particularly the work of Younas et al. [1] on optical solitons in magneto-electro-elastic media, while extending the analytical framework to more complex dispersion relationships. The extended F-expansion technique represents a significant methodological advancement in nonlinear wave analysis, providing a systematic approach that surpasses conventional methods in both computational efficiency and solution versatility. Its applicability extends well beyond the specific case studied here, showing considerable promise for addressing other perturbed integrable systems with higher-order effects. Our analysis reveals the fundamental physical mechanisms through which higher-order dispersion modulates nonlinear wave dynamics. Higher-order dispersion provides additional energy channels that stabilize certain wave structures against collapse or dissipation. The dispersion triplet creates nonlinear coupling between amplitude and phase evolution, enabling sophisticated wave control. These insights directly impact photonic system design, optical communication networks, hydrodynamic modeling, and plasma wave engineering, where precise wave manipulation is crucial. Our analysis provides fundamental insights into how higher-order dispersion mechanisms modulate nonlinear wave dynamics, revealing the intricate balance between nonlinearity, dispersion, and perturbation effects. These findings have important implications for controlling wave propagation in engineered systems, particularly in photonics and fluid dynamics where precise wave management is crucial. The solutions developed accurately model diverse nonlinear behaviors observed in physical contexts including optical fibers, plasma environments, and hydrodynamic systems. Specific applications encompass advanced optical communication systems utilizing soliton propagation, rogue wave prediction in oceanography, and wave engineering in laboratory plasma devices. Through rigorous linear stability analysis and detailed phase-space diagnostics, we have demonstrated the remarkable robustness of the obtained solutions against various perturbation types. Numerical simulations have further validated their mathematical consistency and confirmed their relevance to observable wave phenomena in physical systems. While this work substantially expands the solution space of the Gardner equation, several important questions remain open for future investigation. These include the detailed study of multi-soliton interaction dynamics, the effects of stochastic perturbations on wave stability, and experimental verification of the predicted higher-order dispersion effects. The extended F-expansion technique framework developed here provides a robust foundation for addressing these challenges and can be readily adapted to other non-integrable systems, promising further breakthroughs in understanding nonlinear wave phenomena across different physical domains.

Future investigations will focus on exploring multi-soliton interaction dynamics to understand nonlinear collision processes and energy transfer mechanisms in complex dispersive environments. The development of stochastic frameworks incorporating random perturbations represents another

critical direction, particularly for modeling wave behavior in turbulent physical systems and noisy optical networks. Furthermore, the methodological framework can be extended to nonlocal and fractional Gardner-type equations, enabling the description of long-range interactions and anomalous transport phenomena. From an applied perspective, experimental validation of the predicted higher-order dispersion effects through controlled laboratory setups in optical fibers and plasma chambers remains an essential next step. The integration of machine learning techniques with analytical methods offers exciting possibilities for automated solution discovery and parameter optimization in complex nonlinear systems. Additionally, cross-disciplinary applications in biophysical wave propagation, quantum analogue systems, and environmental prediction models present fertile ground for translating our theoretical advances into practical innovations across multiple scientific domains. These research trajectories not only address natural extensions of our current work but also establish meaningful connections with emerging frontiers in nonlinear science and engineering.

Author contributions

Wafaa B. Rabie: Formal analysis, software, methodology; Hamdy M. Ahmed: Validation, methodology; A. M. Abd-Alla: Writing-review & editing; Khadiga A. Ismail: Resources, writing-review & editing; Ahmed Ramady: Software, investigation. All authors have read and agreed to the published version of the manuscript.

Use of Generative-AI tools declaration

The authors declare they have not used Artificial Intelligence (AI) tools in the creation of this article.

Acknowledgments

The authors extend their appreciation to Taif University, Saudi Arabia, for supporting this work through Project Number (TU-DSPP-2024-81).

Funding

This research was funded by Taif University, Saudi Arabia, Project No. (TU-DSPP-2024-81).

Conflict of interest

All authors declare no conflicts of interest in this paper.

References

1. N. Mhadhbi, S. Gana, M. F. Alsaeedi, Exact solutions for nonlinear partial differential equations via a fusion of classical methods and innovative approaches, *Sci. Rep.*, **14** (2024), 6443. https://doi.org/10.1038/s41598-024-57005-1

2. B. Kopçasız, Unveiling new exact solutions of the complex-coupled Kuralay system using the generalized Riccati equation mapping method, *J. Math. Sci. Model.*, **7** (2024), 146–156. https://doi.org/10.33187/jmsm.1475211

3. M. Jannah, T. Islam, A. Akter, Explicit travelling wave solutions to nonlinear partial differential equations arise in mathematical physics and engineering, *J. Eng. Adv.*, **2** (2021), 58–63. https://doi.org/10.38032/jea.2021.01.008

4. W. B. Rabie, H. M. Ahmed, H. H. Hussein, Novel analytic solutions of strain wave model in micro-structured solids, *Nonlinear Eng.*, **13** (2024), 20220293. https://doi.org/10.1515/nleng-2022-0293

5. W. M. Hasan, H. M. Ahmed, A. M. Ahmed, H. M. Rezk, W. B. Rabie, Exploring highly dispersive optical solitons and modulation instability in nonlinear Schrödinger equations with nonlocal self-phase modulation and polarization dispersion, *Sci. Rep.*, **15** (2025), 27070. https://doi.org/10.1038/s41598-025-09710-8

6. D. M. Gusu, W. Gudeta, Solving nonlinear partial differential equations of special kinds of 3rd order using balance method and its models, *Int. J. Differ. Equat.*, **2023** (2023), 7663326. https://doi.org/10.1155/2023/7663326

7. U. Younas, T. A. Sulaiman, J. Ren, On the optical soliton structures in the magneto electro-elastic circular rod modeled by nonlinear dynamical longitudinal wave equation, *Opt. Quant. Electron.*, **54** (2022), 688. https://doi.org/10.1007/s11082-022-04104-w

8. L. Nottale, Scale relativity and fractal space-time: Applications to quantum physics, cosmology and chaotic systems, *Chaos Soliton. Fract.*, **7** (1996), 877–938. https://doi.org/10.1016/0960-0779(96)00002-1

9. P. K. Shukla, B. Eliasson, Colloquium: Nonlinear collective interactions in quantum plasmas with degenerate electron fluids, *Rev. Mod. Phys.*, **83** (2011), 885–906. https://doi.org/10.1103/RevModPhys.83.885

10. A. Jhangeer, S. Fatima, N. Raza, M. H. Rafiq, N. A. Shah, M. Bayram, Numerical analysis of a novel mathematical model of measles-pneumonia co-infection with treated-vaccinated compartment, *Ain Shams Eng. J.*, **16** (2025), 103659. https://doi.org/10.1016/j.asej.2025.103659

11. U. Akpan, L. Akinyemi, D. Ntiamoah, A. Houwe, S. Abbagari, Generalized stochastic Korteweg-de Vries equations, their Painlevé integrability, N-soliton and other solutions, *Int. J. Geom. Methods M.*, **21** (2024), 2450128. https://doi.org/10.1142/S0219887824501287

12. J. Ahmad, Z. Mustafa, J. Habib, Analyzing dispersive optical solitons in nonlinear models using an analytical technique and its applications, *Opt. Quant. Electron.*, **56** (2024), 77. https://doi.org/10.1007/s11082-023-05552-8

13. J. Ahmad, M. Hameed, Z. Mustafa, F. Pervaiz, M. Nadeem, Y. Alsayaad, A study of traveling wave solutions and modulation instability in the (3+1)-dimensional Sakovich equation employing advanced analytical techniques, *Sci. Rep.*, **15** (2025), 23332. https://doi.org/10.1038/s41598-025-00503-7

14. L. A. A. Essa, M. U. Rahman, Dynamics of bifurcation, chaos, sensitivity and diverse soliton solution to the Drinfeld-Sokolov-Wilson equations arise in mathematical physics, *Int. J. Theor. Phys.*, **63** (2024), 216. https://doi.org/10.1007/s10773-024-05759-9

15. I. Alazman, B. S. T. Alkahtani, M. N. Mishra, Dynamic of bifurcation, chaotic structure and multi-soliton of fractional nonlinear Schrödinger equation arise in plasma physics, *Sci. Rep.*, **14** (2024), 25781. https://doi.org/10.1038/s41598-024-72744-x

16. N. Cao, X. Li, X. Yin, The control model of Rossby waves and dynamic characteristics in stratified fluids, *Chaos Soliton. Fract.*, **201** (2025), 117208. https://doi.org/10.1016/j.chaos.2025.117208

17. J. Muhammad, U. Younas, Wave propagation and multistability analysis to the modified fractional KDV-KP equation in diversity of fields, *Model. Earth Syst. Env.*, **11** (2025), 262. https://doi.org/10.1007/s40808-025-02434-8

18. W. B. Rabie, H. M. Ahmed, T. A. Nofal, S. Alkhatib, Wave solutions for the (3+1)-dimensional fractional Boussinesq-KP-type equation using the modified extended direct algebraic method, *AIMS Math.*, **9** (2024), 31882–31897. https://doi.org/10.3934/math.20241532

19. J. Ahmad, Z. Mustafa, J. Habib, Analyzing dispersive optical solitons in nonlinear models using an analytical technique and its applications, *Opt. Quant. Electron.*, **56** (2024), 77. https://doi.org/10.1007/s11082-023-05552-8

20. B. Ghanbari, D. Baleanu, New solutions of Gardner's equation using two analytical methods, *Front. Phys.*, **7** (2019), 202. https://doi.org/10.3389/fphy.2019.00202

21. S. Kumar, S. Malik, A new analytic approach and its application to new generalized Korteweg-de Vries and modified Korteweg-de Vries equations, *Math. Method. Appl. Sci.*, **47** (2024), 11709–11726. https://doi.org/10.1002/mma.10150

22. S. A. E. Tantawy, W. M. Moslem, Nonlinear structures of the Korteweg-de Vries and modified Korteweg-de Vries equations in non-Maxwellian electron-positron-ion plasma: Solitons collision and rogue waves, *Phys. Plasmas*, **21** (2014), 052107. https://doi.org/10.1063/1.4879815

23. N. Rauf, Mathematical techniques for analyzing nonlinear optical phenomena, *Front. Appl. Phys. Math.*, **1** (2024), 251–285.

24. N. Raees, I. Mahmood, E. Hussain, U. Younas, H. O. Elansary, S. Mumtaz, Dynamics of optical solitons and sensitivity analysis in fiber optics, *Phys. Lett. A*, **528** (2024), 130031. https://doi.org/10.1016/j.physleta.2024.130031

25. W. B. Rabie, H. M. Ahmed, M. Marin, A. A. Syied, A. A. Elmonem, N. S. E. Abdalla, et al., Thorough investigation of exact wave solutions in nonlinear thermoelasticity theory under the influence of gravity using advanced analytical methods, *Acta Mech.*, **236** (2025), 1599–1632. https://doi.org/10.1007/s00707-025-04229-5

26. A. V. Aksenov, A. D. Polyanin, Review of methods for constructing exact solutions of equations of mathematical physics based on simpler solutions, *Theor. Math. Phys.*, **211** (2022), 567–594. https://doi.org/10.1134/S0040577922050014

27. K. Mosegaard, T. M. Hansen, *Inverse methods: Problem formulation and probabilistic solutions*, In: Integrated imaging of the earth: Theory and applications, 2016, 7–27. https://doi.org/10.1002/9781118929063.ch2

28. E. Rivalta, F. Corbi, L. Passarelli, V. Acocella, T. Davis, M. A. D. Vito, Stress inversions to forecast magma pathways and eruptive vent location, *Sci. Adv.*, **5** (2019), eaau9784. https://doi.org/10.1126/sciadv.aau9784

29. A. Bruckstein, T. Kailath, An inverse scattering framework for several problems in signal processing, *IEEE ASSP Mag.*, **4** (1987), 6–20. https://doi.org/10.1109/MASSP.1987.1165567

30. A. F. Alharbi, U. Akram, Ansatz-based exploration of M-shaped and multi-wave solitons in the Kudryashov-Sinelshchikov model, *Mod. Phys. Lett. B*, **39** (2025), 2550169. https://doi.org/10.1142/S0217984925501696

31. W. B. Rabie, H. M. Ahmed, W. Hamdy, Exploration of new optical solitons in magneto-optical waveguides with a coupled system of nonlinear Biswas–Milovic equation via Kudryashov's law using the extended F-expansion method, *Mathematics*, **11** (2023), 300. https://doi.org/10.3390/math11020300

32. L. Kaur, A. Biswas, A. H. Arnous, Y. Yildirim, L. Moraru, M. J. Jweeg, Shock wave and singular solitary wave perturbation with Gardners equation having dispersion triplet, *Contemp. Math.*, **6** (2025), 3743–3762. https://doi.org/10.37256/cm.6320256903

33. A. I. Aliyu, A. Yusuf, D. Baleanu, Optical solitons, conservation laws and modulation instability analysis for the modified nonlinear Schrödinger's equation for Davydov solitons, *J. Electromagnet. Wave.*, **32** (2018), 858–873. https://doi.org/10.1080/09205071.2017.1408499

AIMS Press